University of Pisa
Dept. of Psichiatry, Neurobiology, Pharmacology and Biochemistry
Science of Drug and Bioactive Substances
Prof.ssa Claudia Martini

Antiapoptotic Strategies in Retinal Degeneration: a Biochemical and Functional Approach

A Thesis submitted for the degree of Philosophiæ Doctor by:

Ilaria Piano
(piano@farm.unipi.it)

Under the supervision of:

Prof.ssa Claudia Gargini

March 2011

Declaration

The work described in this thesis is included in the following papers:

MC. Gargini, A. Asta,I. Piano, P. Gasco, C. Musicanti, E. Novelli, E. Strettoi, R. Ghidoni

Inhibition of Ceramide de novo Synthesis in an Animal Model of Retinitis Pigmentosa: Biochemical, Morphological and Functional Effects upon Photoreceptors

CDD Conference 2009 on Neurodegeneration

MC. Gargini, A. Asta,I. Piano, P. Gasco, C. Musicanti, E. Novelli, E. Strettoi, R. Ghidoni

Inhibition of Ceramide de novo Synthesis in an Animal Model of Retinitis Pigmentosa: Biochemical, Morphological and Functional Effects upon Photoreceptors

CDD Conference 2009 on Neurodegeneration

I. Piano, E. Novelli, G. Sala, P. Gasco, C. Gargini, E. Strettoi, R. Ghidoni

The Role of sphingolipids in retinal degeneration

FEBS Advanced Course, Lipid Signalling and Disease-2009

E. Strettoi, R. Ghidoni, G. Sala, E. Novelli, I. Piano, P. Gasco, C. Gargini

Inhibition of Ceramide de-novo sinthesis in animal models of Retinitis Pigmentosa: Rescue effects upon photoreceptors

Retinal International Meeting, Stresa 26-27 June 2010, Italy

I. Piano, E. Novelli, G. Sala, P. Gasco, C. Gargini, E. Strettoi, R. Ghidoni

Sphingolipids in Retinal Degenerations

Sphingolipid Club, Glasgow 30 June-2 July 2010

E. Strettoi, C. Gargini, E. Novelli, G. Sala, I. Piano, P. Gasco, R. Ghidoni

Inhibition of ceramide biosynthesis preserves photoreceptor structure and function in a mouse model of retinitis pigmentosa.

Proc Natl Acad Sci U S A. 2010 Oct 26;107(43):18706-11

Abstract

The sphingolipid ceramide exerts a pro-apoptotic role in variety of cellular and organ systems and increased of de-novo synthesis of ceramide are associated with initiation of cell death. In Retinitis Pigmentosa (RP) photoreceptor death occurs by apoptosis but the individual pathways of this process are unknown. We employed an animal model of RP, the rd10 mutant mouse, to assess the role of ceramide in inherited photoreceptor degeneration. We used Myriocin, a known inhibitor of serine palmitoyltransferase (SPT, the rate-limiting enzyme of ceramide biosynthesis) which was either injected intravitreally in a single dose or administered daily to rd10 mice as eye drops of Solid Lipid Nanoparticles (SLNs). Control mice were given intravitreal injections of vehicle alone or unloaded lipid particles, respectively. We found that retinal ceramide levels in rd10 mice double from P14 to P30, the time interval of maximum photoreceptor death in this strain. Intraocular treatment with Myriocin decreases the number of pycnotic photoreceptors in rd10 mice by approximately 50%. Electroretinogram (ERG) recordings were obtained from animals of various ages chronically treated with Myriocin-SLNs. ERG a-waves persist after P30 in treated mice while these responses are virtually extinct in control littermates. Retinal sections from ERG recorded animals were examined at a confocal microscope to estimate photoreceptor survival. Morphometric analysis of retinas from rd10 mice aged P24 (peak of rod apoptosis) up to P30 showed prolonged survival of photoreceptors in treated animals. This study demonstrates in a mammalian model of RP that it is possible to decrease the rate of apoptotic death of photoreceptors in vivo by lowering retinal ceramide levels through inhibition of the de-novo biosynthesis of this molecule. Non-invasive, chronic administrations of nanoparticles loaded with SPT inhibitors are effective in prolonging survival and light responsiveness of photoreceptors.

Contents

List of Figures

Chapter 1

Introduction

1.1 Retina

Vision is very important in humans because the eye is dedicated to capture light reflected by the scene surronding the subject, to encode it into electrical signals and efficiently transfer them to the brain. A cross-sectional view of the eye shows three different layers:

1. The external layer, formed by the *sclera* and *cornea*
2. The intermediate layer, divided into two parts: anterior composed by *iris* and *ciliary body* and posterior
3. The internal layer that represents the sensory part of the eye, the *retina*.

1.1.1 Morphological structure of the retina

Surrounding the fovea there is a circular area of approximately 6mm in diameter called central retina while beyond this is peripheral retina stretching to the ora serrata that represents the center of the optic nerve. A redial section of the retina shows that the ganglion cells (the output neurons of the retina) lie innermost in the retina closest to the lens and front of the eye, and the photoreceptors (rods and cones) lie outermost in the retina against the pigment epithelium and choroid. A vertical section of the retina is as follows:

- Pigmented Epithelium (PE): placed at the periphery of the retina, is the pigmented cell layer just outside the neurosensory retina that nourishes retinal visual cells, and is firmly attached to the underlying choroid and overlying retinal visual cells. the PE is involved in the phagocytosis of the outer segment of photoreceptors cells and it is also involved in the vitamin A cycle where it isomerizes all trans retinol to 11-cis retinal. PE also serves as the limiting transport factor that maintains the retinal environment by supplying small molecules such as amino acid, ascorbic acid and D-glucose while remaining a tight barrier to choroidal blood borne substances. The ionic enviroment is maintained by a particular exchange system.
- Photoreceptors Layers: contain both Outer and Inner Segment (OS/IS) of the photoreceptors. The OS is the most distal part of photoreceptors and

in this location a multi-stage processe known as phototrasduction begins with light-induced isomerization of a pigment (rhodopsin or cone-opsin). The whole photodrasductive machinery is contained in here. The IS is connected to the OS by a thin cilium, it is the portion of the photoreceptors where most of the biosynthetic processes take place.

- Outer Nuclear Layer (ONL): Contain all the photoreceptors nuclei and the terminal processes of Muller glia.
- Outer Plexiform Layer (OPL): Layer where are synaptical contact between photoreceptors and bipolar cells (second-order neurons).
- Inner Nuclear Layer (INL): Contain the cellular bodies of the all second-order neurons (rod- and cone-bipolar cells, amacrine cells, horizontal cells) and of the non-neural Muller glia.
- Inner Plexiform Layer (IPL): In this layer there are the synaptical contact between second-order neurons and ganglion cells.
- Ganglion Cell Layer (GCL): Contain both ganglion cell and displaced amacrine cellular bodies. Ganglion cells represent the third-order neurons, the only neurons generating both spontaneus and light-evoked spike potentials.
- Optic Nerve Fiber Layer (NFL): It's the output of the axon of the ganglion cells to the brain. Packed together they form the optic nerve and at the level of optic disc assumes the usual myelination.

1.1.2 Retina of the Mouse vs Human

In the mouse retina we can recognise the same layer of the human retina. The mouse retina is rod-dominated (rods 4.5milion versus cones 125.000) and at variance with human retina there aren't three type of cones but only two: green and blu cones. Similarly to those of humans, photoreceptors of the rodents, rods and cones, absorb photons and convert them into electrical signals. Dim light signals have sufficient energy to excite the rods, while cones are less sensitive and to be excited require much brighter lights. Therefore rod photoreceptor cells operate in the twilight while cone visual cells are active at daylight and subserve color vision. Photoreceptor cells may be connected to the neighboring cells by electrical synapses (gap junctions) and establish chemical synapses with bipolar and horizontal cells. Bipolar cells are subdivided into two main classes: rod and cone bipolar, each bipolar cells make contact with the corresponding photoreceptor populations. Cone bipolar cells are furhter divided in two subtype: ON- and OFF-bipolar cells, that respectively depolarize and hyperpolarize in response to the illumination of their receptive field centers. All rod-bipolar cells are of subtype ON and establish direct connection with ON ganglion cells (RGC) through amacrine cells. Both ON- and OFF cone-bipolar cells are connected directly to respectively ON or OFF RGCs.

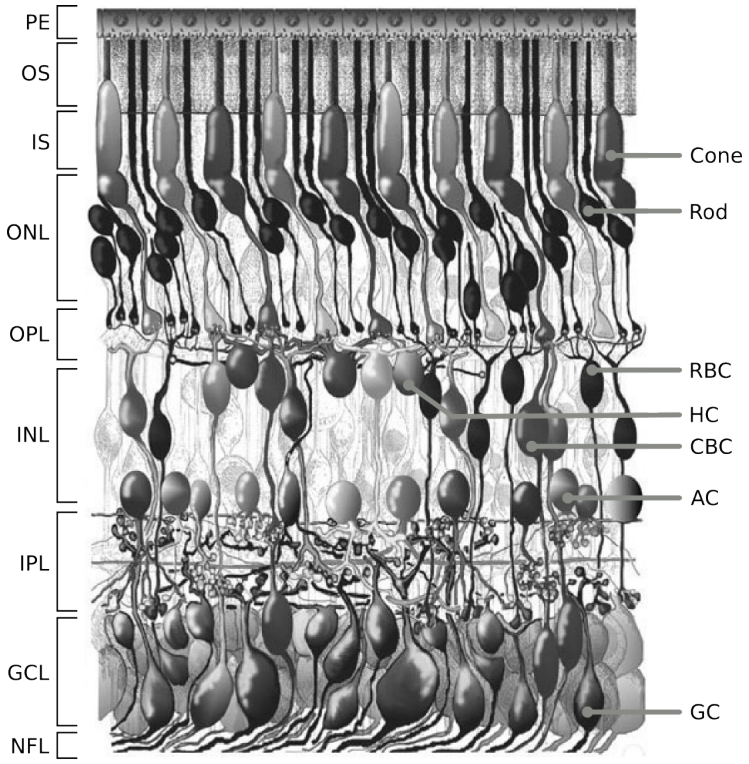

Figure 1.1: Morphological representation of the retina in a vertical section of the adult human eye. Retinal layers on the left. Principal neuronal classes on the right. RBC: rod bipolar cell, HC: horizontal cell, CBC: cone bipolar cell, AC: amacrine cell, GC: ganglion cell

1.2 Retinal Degenerations (RDs)

A very high number of genetic mutations affect the eye and a large number of mutations affect photoreceptors or pigment epithelium and may cause retinal degeneration (RDs). Retinitis Pigmentosa (RP) comprises a group of heterogeneus genetic disorders that cause severe loss of vision in as many as 1.5 milion individuals worldwide (review: [68], [44],[81]). The mutation mainly affects the rod photoreceptors which mediate the scotopic vision (dim light conditions). When rods start to die, in response to genetic abnormality, symptoms appear and the night vision of patients is reduced and the visual field is constricted (tunnel vision). RP usually follows a two-stage process in which first the rod-photoreceptors degenerate, then also cone-photoreceptors start to die resulting in the loss of central vision. At this stage of RP also blood vassel distrophy and intraretinal brown pigment accumulation occur. It is unusual for patients with RP to became totally blind as most of them retain some useful vision well into old ages. Type of RP and related diseases include, among others, Usher syndrome, Leber's congenital amaurosis, rod-cone disease, Bardet-Biedl syndrome and Refsum disease.

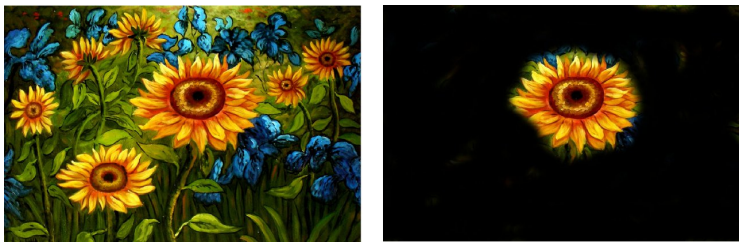

Figure 1.2: The progressive die of the rod-photoreceptors lead to loss of peripheral vision.

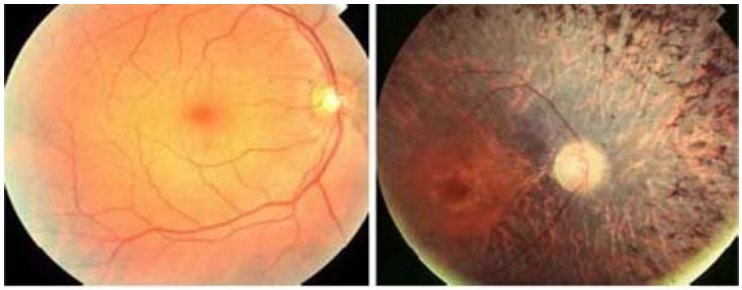

Figure 1.3: A typical brown pigmentation is present in the pathological condition. Pigment deposits, named bone spicules for their shape, are responsiblefor the name of the disease. In these image is also visible a clear attenuation of retinal blood vassels.

1.2.1 Retinitis Pigmentosa: Genetics and Molecular Mechanisms

There are three principal types of RP: autosominal dominant (ad), autosominal recessive (ar) and X-linked. RP causing mutations have been identified in more than 35 genes. Genetic mutations (as deletions, insertions, or substitutions) triggering potoreceptors degeneration and then death by apoptosis, often affect the retinoid acid cycle or the phototransduction cascade. Phototransduction starts with a light-induced, conformational change of 11-cis-retinal to all-trans-retinal. This in turn activates opsin molecules, causing sequential activation of transducine and cyclic guanosine monophosphate (cGMP)-phosphodiesterase-6 (PDE6) and subsequent decreases in intracellular cGMP concentration. High cGMP levels maintain cyclic nucleotide-gated (CNG) cation channels in the open state, allowing the influx of cations including sodium and calcium. Reduction of cGMP levels closes CNG channels causing cell hyperpolarization. This signal is then transmitted to second order neurons in the INL Fig.1.4 ([68]).
There are mainly two mutations affecting the phototransductive process: the first concerns, the Rhodopsin gene (RHO), this is the best studied mutation and is responsible for varius forms of autosominal dominant RP (adRP); the second, that affects the phosphodiesterase gene (Pdeb), leads to autosominal recessive RP (arRP) and this is the defect carried by the mouse models used in the present study (explained in more detail later).

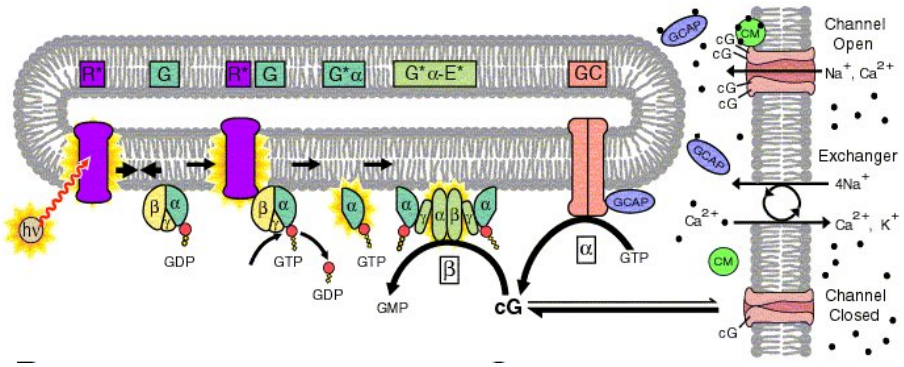

Figure 1.4: Pathway of the visual transduction cascade.

1.2.2 RHO Mutations

Rhodopsin is a prototypic member of the G-protein-coupled receptor family and its molecular structure has been known for some time ([79],[80]). The visual pigment molecule consists of a protein component (a 348 amino acid sequence organized into three distinct domains: cytoplasmic, transmembrane and intradiscal), and chromophore group (11-cis-retinal a light absorbing polyen structure where phototransduction initiates, fig.1.4) The most common mutation in RHO gene is the change of proline to histidine at codon 23 (P23H), this mutation leads to a phenotype classified as class B1 with a typical features that includes slower progression and better visual function compared to other forms of adRP. Besides P23H, there are several other types of mutations in the RHO gene that are classified as follows:

- Class I: mutations basically occur in the C-terminus of the protein, this part of the protein is important for its translocation to the plasma membrane and could form a functional chromophore with 11-cis-retinal.
- Class II: the most common adRP mutations, were characterized by mutations in the intradiscal membranes and cytoplasmatic domain of rhodopsin, which resulting in misfolding of the protein, defined by the inability to form a functional chromophore with 11-cis-retinal.
- Class III: corresponds to mutations that affect endocytosis (R135L mutation).
- Class IV: these mutations affect the rhodopsin stability and post - translational modification, such as T4R mutation that causes adRP in dogs.
- Class V: have no abvius initial folding defect but show an increased activation rate of for transducin.
- Class VI: this mutant appears to fold correctly bat leads to the constitutive activation of opsin in the absence of chromophore and in dark.

Dominance in adRP patients could be due to loss-of-function, gain-of-function or dominant-negative mutations, or any of the above in combination.

Several animal models of rhodopsin-associated RP have been generated and include the rhodopsin knockout mouse lacking any functional rhodopsin and thus rapidly undergoes retinal degeneration, and dominant transgenic models such as the P23H mouse ([77]). These animals are an extremely valuable resource in the study of rhodopsin-induced degeneration mechanisms.

1.2.3 Mutations in photoreceptor structural proteins

Several of the known RP genes encode proteins that have pivotal roles in the formation and maintenance of the highly complex and delicate cellular structure of the rod (Fig.1.5). Peripherina 2 also known as retinal degeneration slow

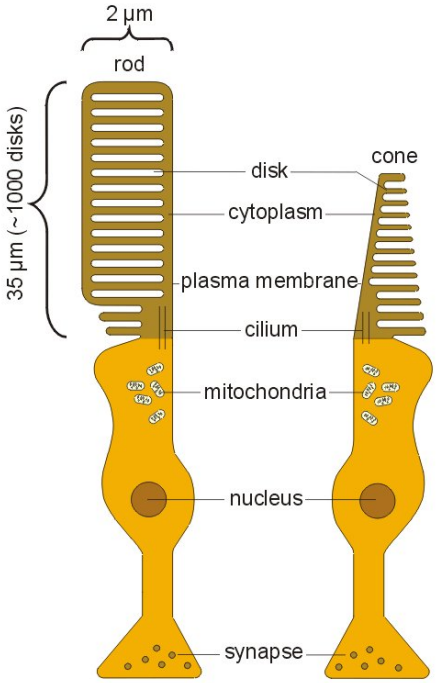

Figure 1.5: This figure show a schematic representation of the complex photoreceptor strcture.

(RDS), a transmembrane glycoprotein, is one of the earliest proteins to be associated with RP. Mutations in RDS lead to several different retinal phenotypes including arRP, cone-rod dystrophy and adRP
(http://www.sph.uth.tmc.edu/Retnet/home.htm).
RDS estabilishes complexes that have an integral role in the morphogenesis and structure of the stacked discs in both rod and cone OS (see fig.1.5). RDS mutations lead to RP by two different mechanisms. First, alterations prevent the protein from forming tetramers, inhibiting its transportation from the translation site in the IS to the OS; second, the mutant protein is incorporated into the nascent disc but causes them to be inherently unstable and RP develops because of the disorganization that ensues in the OS ([26],[42], [57]). Mutations in the RP1 gene are among the most common causes of adRP and are responsible

for 6-10 per cent of cases. The role of the RP1 protein might be central to the morphogenesis of the photoreceptors OS ([107]).

1.2.4 Abnormalities in retinal transcriptional factors

The process that occurs in development, differentiation and maintenance of the photoreceptors are under the control of several transcription factors, such as cone-rod homeobox-cointaining (CRX) and neural retina leucine zipper (NRL) genes. CRX is essential for photoreceptor development and when mutated is associated with the early onset retinal degeneration laber congenital amaurosis (LCA) and adRP; NRL is pivotal in the determination and development of the photoreceptors and also in their function and maintenance in the adult, in patients with NRL mutations, it appears that the detrimental effects might be a result of increased expression of rhodopsin and other photoreceptor gene ([17]).

1.2.5 Rod-phosphodiesterase (PDE) gene mutations

Several forms of the arRP are caused by mutations carried in the PDE gene. Cyclic GMP-phosphodiesterase is composed of four subunits, two with catalytic activity, α and β, and two identical gamma subunits with inhibitory activity. This enzyme is fundamentally important for phototrasduction in photoreceptors ([25]).
cGMP phosphodiesterase type 6 (PDE6) is the specific enzyme in rod-photoreceptor. PDE6 is activated in response to light stimulation of the receptor in the outer segments of rod (Fig.1.4). A visual cascade of biochemical reactions is initiated when rhodopsin is activated by the incident light. Activated rhodopsin stimulates the exchange of GDP for GTP and activates the G-protein, transducin. Transducin activates PDE6 by displacing the inhibitory γ-subunits from the active site of the enzyme, thereby greatly stimulating cGMP hydrolysis. PDE6 rapidly reduces the cytoplasmic cGMP concentration, which causes closure of cGMP-gated channels and produces a transient hyperpolarization of the rod plasma membrane leading to a reduction in glutamate release at the synapse ([40]).
In 1924 Keeler and collaborators discovered for the first time the mutations in the PDE gene in rodless mice (r) ([43]), this were a nonsense mutation in the PDE gene coding for the beta-subunit of cGMP phosphodiesterase gene.This spontaneus mutation was later rediscovered in the retinal degeneration mouse (rd1 or rd)([9],[84], [85], [86]) and subsequently in humans with arRP and adRP form of night blindness ([66], [65], [28]).
Mouse model of retinal degeneration has been investigated for many years in the hope of understanding the causes of photoreceptors cell death. The first retinal degeneration observed is *rd1*. This mutation has been found among several common laboratory strain (such as C3H and CBA/J) and mice homozygous for the *rd1* mutation have an early onset severe retinal degeneration due to a murine viral insert (MLV) and a second nonsense mutation in exon 7 of the *Pde6b* gene enconding the beta subunit of cGMP-PDE. Mice with the *rd1* mutation can be easily typed by phenotype based on vassel attenuation and pigment patches in the fundus (Fig.1.6) ([14]).
Biochemical studies comparing retinas from wt and *rd1* mice have shown that the lack of cGMP-PDE activity causes a dramatic increase in cytoplasmatic

Figure 1.6: This image show the appearance of the ocular fundus in the *rd1* mice retina.

cGMP concentration, this, in turn, leads to a permanent opening of the cGMP gated cation channels on the photoreceptor membrane with an increase of the extracellular ions influx, particularly Ca^{2+}. It has been suggested that this increase in intracellular Ca^{2+} causes a metabolic overload of the cells, eventually leading to cell death by apoptosis ([16]). Excessive Ca^{2+} influx has long been regarded as a major factor in photoreceptor degeneration and strong activation of Ca^{2+}-dependent enzymes has been observed in *rd1* photoreceptors. Certainly, Ca^{2+} is seen as a trigger of apoptosis through the inactivation of mitochondria and subsequent activation of apoptotic machinery. On the other hand, Ca^{2+} influx causes ATP depletion by activating Ca^{2+} extrusion mechanisms such as Ca^{2+}-ATPaese or the Na-ATPases required to drive Na^{+}/Ca^{2+} exchangers, while at the same time inhibiting mitochondrial ATP synthesis. A possibility is that the observed rise in retinal Ca^{2+} levels is only secondary to the degeneration process and it is not even clear whether it occurs in photoreceptors or in other retinal cell types. Furthermore, fluctuations in cytosolic Ca^{2+} may be caused not only by Ca^{2+} influx from extracellular sources bat also by intracellular release from the mitochondria, photoreceptor discs or the endoplasmatic reticulum (ER). Further, other mechanisms can lead to cell death such as oxdative stress and activation of the proapoptotic protein. In summary Ca^{2+}, the energetic status, and ER stress are different factors that appear to be interconnected in cell death: a primary rise in intracellular Ca^{2+} triggered by ER stress could be followed by mitochondrial dysfunction, an energetic collapse, and a secondary wave of extracellular Ca^{2+} ([90]).
In addition to *rd1* mouse model, other naturally occuring mouse mutants that manifest degeneration of photoreceptors in the retina with preservation of all other retinal cell types have been found such as:

- Purkinje cell degeneration (*pcd*)
- nervous (*nr*)
- retinal degeneration slow (*rds*)
- motor neuron degeneration (*mnd*)

- vitiligo (*vit*)
- neuronal ceroid lipofuscinosis (*nclf*)
- cone photoreceptor function loss (*cpfl1*)
- and several types of retinal degeneration (*rd3*, *rd4*, *rd5*, *rd6*, *rd7*, *rd8*, *rd9* and *rd10*) ([14]).

1.2.6 The rd10 mutant mouse

Retinal degeneration 10 (*rd10*) mouse is a viable model of human retinitis pigmentosa and this strain is used in the present study. Genetic analysis shows that these mice carry an autosomal recessive mutation that maps into chromosome (Chr) 5. Sequence analysis shows that the retinal degeneration is caused by a missense point mutation in 13^{th} exon in the *Pde6b* gene of the beta-subunit of the rod cGMP phosphodiesterase (beta-PDE). The mutation changes codon 560 from CGC to TGC resulting into an arginine to a cysteine. The exon 13 missense mutation is the first known occurence of a remutation in the *Pde6b* gene in mice and provide a good model for studying the pathogenesis of arRP in human. It also provides a better model than *rd1* for experimental pharmaceutical-based therapy for RP because of its later onset, slowly progressing and less severe retinal degeneration compared to that affecting the *rd1* ([14]).
In the *rd10* mice the number of photoreceptor rows is 12-14 at postnatal day 10 (P10) and 11-12 rows at P20. From P20 to P25 there is a substantial reduction in the number of photoreceptor rows and at P30 cones are shortened outer and inner segmented and a deformed shape. At P45, only a single row of photoreceptors is present (Fig.1.7). Degeneration of photoreceptors in *rd10* retinas follows a center-to-periphery gradient: the decrease in the number of ONL rows becomes apparent in the central retina first, whereas degeneration in the periphery is delayed ([29]). Atrophic retinal vessels are found at four weeks of age, consistent with retinal degeneration ([15], [29]). After extensive photoreceptor death, dendrites of the bipolar cells exhibit a retraction. Survival of rod bipolar and horizontal cells drops right after the peak of photoreceptor degeneration and decreases slowly over the following months. After that, also the INL disorganizes and typical rosettes appear.
The morphological changes have a physiological correlate. Infact elettroretinogram (ERG) analysis shows differences between the flash ERG of wt and *rd10* mice related with severe damage affecting the distal rod pathway. The loss of functioning rods that occurs in the *rd10* mutants between P20 and P30 largely contributes to the drastic reduction in the normalized maximal a-wave that is directly proportional to the suppression of the dark current by light ([10]). Note that alterations in the shape and relative amplitude of the b-wave are detected as early as P18 when no morphological modification occur in inner retina. Changes in the efficiency of the synaptic communication of rod-to-rod bipolar cells could explain the alterations found in the ERG by using sinusoidal stimuli. In fact the ERG mesurements obtained by using sinusoidal modulation of the mean luminance confirm the results of the flash ERG, and provide an indication that, even at earliest stage of the degenerative process, bipolar neurons show signs of damage ([29]).

1.2.7 Secondary cell death of Cone-photoreceptors

Photoreceptor degeneration results in vision loss in diseases like RP and age-related macular degeneration. In these diseases, the main cause of clinically significant vision loss is cone cell degeneration rather than rod cell death. In fact most mutations responsible for RP in humans and animal models affect rod-photoreceptor-specific genes, rod apoptosis is often followed by secondary cone degeneration ([71]). Several possible causes have been indicated to explain mutation-indipendent secondary cell death of cone-photoreceptors. These include loss of structural support and/or loss of trophic support, i.e, Rod-derived Cone Viability Factor (RdCVF) ([89]) when rod negatively affect the cells are degenerating and death. In fact, intraocular injections of this factor may to rescue cone photoreceptors ([112]).
Another hypothesis concerning the changes in oxigen consumption levels as a function of rod degeneration: depletion of the photoreceptor population (mainly rods) by any cause would reduce consumption of oxygen flowing from the choroidal circulation. Because this flow of oxygen is unregulated, photoreceptor depletion will cause a chronic increase in oxygen tension in the outer retina, and this increase is toxic to surviving photoreceptor (both rods and cones) ([18]). The vulnerability of photoreceptors to hyperoxia has also been confirmed, and evidence has been reported that rod loss results in oxidative stress to cones ([94]).
Two other hypothesis have recently been developed concerning the secondary death of cones: rods may release toxic substances that negatively affect the neighboring cells and a chronic activation of microglial cells has been described in animal models of RP. It is possible that an immune response might enhance degenerative processes and could in part be responsible for the secondary loss of cone-photoreceptors which are not affected by the primary genetic mutation ([113]).

1.3 RP experimental therapeutic strategies

1.3.1 Transplants

The possibility of retinal transplantation represents a hope for the restoration of vision through cell-replacement therapy. However, getting the transplanted cells to establish the right connections within the retina has been a major problem by far. It appears that an early developmental stage of the retina of acceptors represents a key feature of a successful transplant. Despite decades of experimental attempts, transplants have yet to produce better vision in mammals with retinal degeneration because the transplanted cells do not wire up properly. The first successful transplant of a mammalian retina dates back to 1959, when Royo and Quay transplanted fetal rat retinas into the eyes of adults of the same strain. Transplants appear to develop many characteristics of a normal retina ([93]; [115]) and grow to form a second retinal layer underneath the host tissue. Further, transplant of microaggregates containing clumps of few retinal neurons from newborn mice, develop most characteristics of rod photoreceptors including the expression of the rhodopsin and the outer segments ([32], [33]). Unfortunately, both these type of transplantion remain isolated without interacting or integrating effectively with the host retinal neurons. On the contrary,

integration with the host retinal neurons is obtained when transplanting retinal stem cells derived from fetal or newborn mice or rats, or from human fetuses. In fact, when these cells are transplanted into both normal and degenerating retinas migrate into all retina layers and develop morphological characteristics of several retinal cell types, mainly photoreceptors ([13], [19], [46]). There is also evidence to show that the best donor cells should be from 3 to 5 days old, approximately two or three days after the peak of rod photoreceptor development in the mouse retina. This suggests that, newly born rods, rather than the stem cells, are the best candidates for cellular transplantation ([61]).
On a different rationale, promising results for RP treatment have been obtained, still using a cell-based approach ([78]). These study have shown that injections of hematopoietic stem cells (lineage-negative called Lin-HSCs) into the eye of mouse models of RP (rd1 and rd10 mice) result into a dramatic rescue of both blood vessels and photoreceptors, mainly cones. These mice show an improvement of the ERG at an age when usually it is completely extinct and the rescue effects are long lasting.

1.3.2 Implants: Subretinal and Epiretinal prostheses

The development of artificialimplants inserted in substitution of an entire part of the pathological retina represents an active line of investigation to treat both RP and other retinal diseases, such as macular degeneration. Advances in microtechnology have facilitated the development of a variety of prostheses that can be connected to the brain or implanted in the eye; these implants have a greater potential for visual restoration as they are well tolerated and remain viable for several years; on the on the hand, retinal prostheses are only effective where the visual pathway distal to the retinal implant is still functional. Two types of prostheses have been developed: subretinal and epiretinal (Fig.1.8). Subretinal prostheses contain microphotodiodes attached to micro-electrodes. These implants, such as the articial silicon retina (5000 micro-electrodes), are placed in the subretinal space between the outer retina and retinal pigment epithelium (Fig.1.8). The photodiodes are stimulated by light pass- ing trough the retina, and the resulting electric current excites adjacent retinal sensory neurons. These implants do not require an external electrical source as incident light is sufficient for stimulation ([116]). Preclinical evaluation shows that several species of the animal have a tolerance to the implants up to 30 months, and histological examination does not show significant changes in the morphology of the retina. In six patients with RP, who received a subretinal implants, visual perception but also appreciation of brightness, contrast of color, movement, shape and vi- sual eld are improved. Some patients showed also an improvement in visual acuity. Two major advantages of subretinal prostheses are the utilization of existing forces between the neural retina and retinal pigment epithelium to maintain their position and the potential of a high spatial resolution, as they are posi- tioned close to retinal nerve cells and can stimulate neurons by means of low electrical currents. The main disadvantages of subretinal implants include im- paired nourishment of the inner retina due to the creation of a mechanical barrier between the outer retina and the choroid and the occurrence of trauma to the retina during the implanting. These prostheses also show poor dissipation of heat and therefore could damage the retina. The mechanism of action of these implants may be by direct stimulation of retinal neurons. A specific

neurotrophic eect elicited locally onto photoreceptors by means of the surgical procedure cannot be excluded: a study of subretinal artificial silicon implants in rats showed a temporary protective eect on the retina, resulting in increased generation of photoreceptors.
Epiretinal prostheses are composed of an array of electrodes implanted on the surface of the retina between the vitreous and inner limiting membrane. The implants receive electrical signals from a camera positioned outside the body (Fig.1.8); the camera transmits light signals to a microchip within the camera. After that, the microchip decodes the signals and relays it, by wireless transmission, to a microchip in the epiretinal implant that in turn stimulates the RGCs ([116]). Clinical trials in humans have reported simple visual perception as phosphenes; these implants have survived up to two years.
Respect to subretinal implants, an advantage of epiretinal devices is that the camera can process signals before they reach the implant: this allows optimization of the signal quality that leads to improved visual perception. Epiretinal implants can also use the heat dissipating properties of the vitreous and are therefore less likely than subretinal implants to damage the retina. The supercial location of the epiretinal devices reduces risk of trauma during both implantation and replacement. The principal disadvantage of epiretinal implants, compared to subretinal devices, is the complicated microtechnology and surgical techniques for a secure xation of the implant on the retina; furthermore, the epiretinal implants requires a higher electrical current than the subretinal implants, and these devices are being developed to generate their own currents on stimulation ([50]).

1.3.3 Neuroprotective factors

Most mutations responsible for the RP phenotype selectively affect rod photoreceptors, however cones undergo degeneration secondary to the loss of rods, often leading to total blindeness. How to save the cones has become a major research challenge because preserving 5 % of all cones may be sufficient to maintain a useful vision, and 50 % of cone functionality would ensure a normal visual acuity. Treatment with neuroprotective factors, such as brain-derived (BDNF), ciliary (CNTF), or glial cell line-derived (GDNF) neurotrophic factor, has been found to protect partially against photoreceptors degeneration in several animal models ([24], [51], [97]). Further, neuroprotective factors could work indipendently of the genetic mutation that cause RP, and therefore could bypass the very high genetic heterogeneity of this disease. CNTF, initially identified as a factor in chick embryo extract that supported viability of embryonic chick ciliary neurons ([2], [105]) and later purified to homogeneity, exhibits multiple biological effects in the retina ([55], [102]). CNTF promotes the survival and axonal regeneration of retinal ganglion cells ([108], [41], [69]) and acts as neuronal differentiation factor, promotes the differentiation of cone photoreceptors expressing green opsin in the developing chick retina ([27], [45], [111]), enhances the expression of bipolar neuron markers in rat retinal cultures and inhibits rod photoreceptor cell differentiation ([6], [23], [72], [92]), and promotes Muller glia genesis from the postnatal retinal progenitor pool ([34]). It has been reported that CNTF regulates the photodrsduction machinery of rod photoreceptor, and the regulation was mediated through Muller cells ([109], [110]).
A recent study ([53]) shows that delivery of CNTF preservs cone cells and their

function stimulating regeneration of COS. In the early stages of degeneration, cone without COS are not only alive but are capable of regenerating their outer segments (woithout COS, cones lose their light-sensig funcion), indicating that at this time the degeneration process is reversible. They found that the delay between loss of COS and cell death is likely in the time frame of about two months in their animal models. Considering the rapid rod degeneration (about 10 days) in these animals, the secondary cone degeneration was relatively slow process, which not only provides an opportunity to study the patology of secondary cone degeneration, but also serves a model for preclinical assessment of potential treatments. Further, this finding araises the possibility that a similar window may exist in patients with RP, in order to allow therapeutic intervention to save cones.
The importance of rod-cone interactions for cone survival was suggested subsequent to the identification of the first causal mutations in RP ([22], [83]). The rod dependence of cone survival is also supported by the experiments *in vitro* ([38]) and by the studies of transgenic mice and mutant zebrafish ([39], [30]), suggesting cell-to-cell interactions in photoreceptor degeneration. RdCVF was isolated for its effect on cone survival using embryonic chick cone cultures ([60]). The effect of the injections of RdCVF protein from old mice 6 to 8 months indicates that this factor induces cone survival directly but does not act indirectly by stimulating rod survival, as most rods have already degenerated at the time of treatment. This trophic effect appears indipendent from the mechanisms of rod degenaration and thus of the causal mutation when the mutated gene is only expressed in rods. RdCVF induces also a functional rescue, thus validating the potential of this trophic factor for therapeutic applications, and in adressing the secondary degeneration of cones, RdCVF administration may be used to target a pathological mechanisms common to most forms of the disease. A recent study on the P23H rat suggests that RdCVF administration may be efficient in the treatment of autosomal dominant RP due to rhodopsin mutations, which account for 30-40% of cases of human autosominal dominant RP ([112]).

1.3.4 Gene therapy

Cone cell bodies remain present longer than rods in both humans and animals, but these light-insensitive cells can be reactivated for a significant time window after the loss of photosensitivity. Another recent study ([11]) shows that a microbial gene introduced to surviving cone cell bodies reactivated retinal ON and OFF patways and the retinal circuitry for lateral inhibition and directional selective responses. The reactivated cones enabled RD mice to perform visually-guided behaviors. The tested time window of intervention suggests that persisting cone cell bodies (about 25%) was enough to induce ganglion cell activity, even during later stages of degeneration.

1.3.5 Antioxidant agents

Another possible explanation for the slowly progressive death of cones after the death of rods, in RP, is oxidative damage. The demostration that oxidtive damage contributes to cone cell death in RP has important clinical implications. It provides a therapeutic target that may apply to all RP patients. The enormous genetic heterogeneity among the diseases that constitute RP is a problem for

the development of treatments that deal with primary genetic defects. If, regardless of the genetic defect that leads to rod-cell death, the same treatment can be used to prolong cone survival and function with an enormous impact. As long as cones survive, useful vision is possible and, although it would be ideal to salvage rods as well, it is not necessary, because patients can carry on relatively normal lives with only cone function.
In varius animal models, three agents, α-tocopherol, ascorbic acid, and α-lipoic acid,have been shown to reduce one or more types of oxidative stress ([12], [98], [73], [49], [82]), and these agents may have additive effects when used together ([100]). Another potent antioxidant that is adept at reducing oxidative damage in mitochondria, MnTBAP, does not cross the blood-brain or blood-retinal barriers under normal circumstances ([67]), but because the blood-retinal barrier in compromised in RP, MnTBAP was also added the regimen. Daily systemic injections of the mixture starting at P18 in rd1 mouse, the time of onset of cone cell death, reduced staining for acrolein (marker of oxidative damage) in cones at P35 to undetectable levels, indicating that the treatment reduced oxidative damage in cones.
Further, an additional support for the hypothesis that oxidative stress is an important contributor to cone cell death in RP, is shown in Komeima et al. ([48]), they found that compared to paired vehicle controls, daily administration of either α-tocopherol or α-lipoic acid as monotherapy also reduced in a significant increase in cone cell number at P35 in rd1 mice.
Combining this approach with other strategies designed to bolster components of the endogenous defense system directed against oxidative stress, as well as enhancing levels of survival factors, may be needed to provide manigful benefit with RP.

1.4 Sphingolipids: Role in RP

Complex sphingolipids are composed of bioactive backbones (sphingoid bases and ceramides) that can cause cell death when the amounts are elevated by turnover of complex sphingolipids, disruption of normal sphingolipids metabolism or induction of sphingolipid biosynthesis *de novo*.
Sphingolipid biosynthesis produces several bioactive intermediates formed from complex sphingolipid turnover: ceramides, sphngoid bases (sphingosine and sphinganine) and sphingoid base 1-phosphates ([36]). The principal enzymes of sphingolipid turnover are sphingomyelinase and ceramidases but there are at least six key enzymes that partecipate in the *de novo* pathway that form/remove these compounds: serine palmitoyltransferase (SPT), which catalyzes the first reaction of the pathway; ceramide synthase, the enzyme responsible for trapping sphinganine as dihydroceramides; dihydroceramide desaturase, which converts dihydroceramides to ceramides; and enzymes such as sphinganine kinase, sphingomyelin synthase, glucosylceramide synthase, etc. which remove or modify these intermediates ([56]).
Ceramide, a sphingolipid metabolic precursor, is a bioactive lipid that has been proposed to be an endogenous mediator of apoptosis; ceramide is actively involved in the triggering of apoptosis in many cell systems, including neurons. Increased intracellular levels of ceramide have been shown to occur during hypoxia, trophic factor removal, treatment with chemotherapeutic agents, heat,

UV radiation, and other stress signals, such as oxidative stress ([31]). Ceramide levels depend on the activity of several enzymes that participate in its synthesis and catabolism. The increase in ceramide in response to apoptotic stimuli may arise from hydrolysis of sphingomyelin due to stimulation of sphingomyelinases, through *de novo* biosynthesis, or from the combined stimulation of both pathway ([8]). In turn, several biochemical reactions lead to the disappearance of ceramide: its hydrolysis catalyzed by ceramidases, sphingomyelin resynthesis, or ceramide glucosylation.
Only recently, it was demonstrated for the first time that the sphingolipid pathway is involved in photoreceptor apoptosis in *Drosophila* ([1]), and a mutation in a novel ceramide kinase gene has been recently established as a cause of an autosomal recessive form of RP, suggesting a direct link between sphingolipid-mediated apoptosis and retinal degeneration ([104]).

1.4.1 How the Ceramide works?

The *de novo* synthesis of ceramide occurs in the endoplasmatic reticulum (ER) and in mitochondria ([62], [96]). In recent years, ceramide has become increasingly appreciated as a bioactive lipid that modulates apoptotic/necrotic cellular processes that are integrated at the mitochondrial level, while sphingosine-1-phosphate has been shown to be protective/anti-apoptotic. In fact, it has been proposed that it is the ratio of sphingosine-1-phosphate to ceramide/sphingosine that determines the fate of a cell ([20], [76]);
There are a number of observations that support a proapoptotic role for ceramide in apoptosis:

- First, ceramide generation is a common cellular response of a variety of cell types following exposure to apoptosis-inducing agents ([75]);
- Second, the effective doses of these agents required to induce ceramide generation closely matches the dose required to induce apoptosis ([47]);
- Third, elevations in cellular ceramide addition in response to these agents occurs prior to the execution phase of apoptosis ([35], [7]);
- Fourth, exogenous addition of cell-permeable ceramide analogues induces apoptosis in a variety of cell lines ([75]);
- Fifth, ceramide-induced apoptosis is very specific, as a naturally occurring ceramide precursor dihydroceramide does not induce apoptosis ([75]);
- Sixth, apoptosis can be inhibited upon blockage of ceramide generation and cells that are incapable of generating ceramide are often incapable of undergoing apoptosis ([3], [88]).

Furthermore, ceramides have been reported to have numerous effects on mitochondria, including enhanced generation of reactive oxygen species, alteration of calcium homeostasis of mitochondria and ER, ATP depletion, collapse in the inner mitochondrial membrane potential, inhibition and/or activation of the activities of various components of the mitochondrial electron transport chain and release of intermembrane space proteins. Further, it has been suggested that ceramide conveys death signals to mitochondria by two principal mechanisms:

1. ceramide leads to a selective permeabilization of the outer mitochondrial membrane for proapoptotic proteins as a process independent of inner membrane functions;

2. the second mechanisms presumes that loss of the permeability barrier of the inner mitochondrial membrane is a prerequisite for the subsequent outer membrane permebilization.

Participation of the inner mitochondrial membrane in the release of proapoptotic preoteins involves the obligatory opening of the Permeability Transition Pore (PTP) in the inner membrane. PTP opening occurs as a result of direct interaction of ceramide with the pore in the presence of Ca^{2+} or that PTP opening follows mitochondrial Ca^{2+} overload. Support for this mechanism arises from experiments with many cell types in which ceramide-induced cell death is suppressed by PTP inhibitors, such as cyclosporina A and bongkrekic acid ([99], [54]). Models of mitochondrial Ca^{2+} overload as a consequence of ceramide-induced Ca^{2+} release from ER and the direct activation of PTP by ceramides where largely based on data obtained using artificial C_2-ceramide ([74]).

1.4.2 De Novo ceramide biosynthesis enzyme and its Inhibitor

The first demostration of toxicity owing to alteration of *de novo* ceramide biosynthesis was the discovery that fumonisins inhibit ceramide synthase ([63]). Further, it is possible that many factors that perturb intermediary metabolism affect sphingolipid biosynthesis and thereby alter the amounts of sphinganine, ceramide, etc. as shown in Fig.1.11. It has been shown that some aspects of the toxicity of palmitate for cells in culture is due to sphingolipid biosynthesis and the overexpression of Serine palmitoyltransferase (SPT) can also induce apoptosis ([95]). SPT is a pyridoxal 5'-phosphate-dependent enzyme that condenses serine with palmitoyl-CoA to produce 3-ketosphinganine (Fig.1.12). For mammals and yeast, two gene products (SPT1 and SPT2) are necessary for activity and appear to be associated physically.
Because SPT is a key enzyme for the regulation of sphingolipid levels in cells, the specific inhibitors of SPT are useful for understanding the physiological roles of sphingolipids. Several natural and synthetic inhibitors of SPT have been reported. ISP-1 (Myriocin) from a culture of fungus *Isalia sinclairii* is a widely used and highly selective SPT inhibitor. The structure of myriocin resembles that of sphingosine (Fig. 1.12). Myriocin inhibits ceramide synthesis in mammalian cells with IC_{50} values in the nanomolar range, while a micromolar concentration of myriocin is necessary for the inhibition of sphingolipid synthesis in *S. cerevisiae* ([70], [103]).

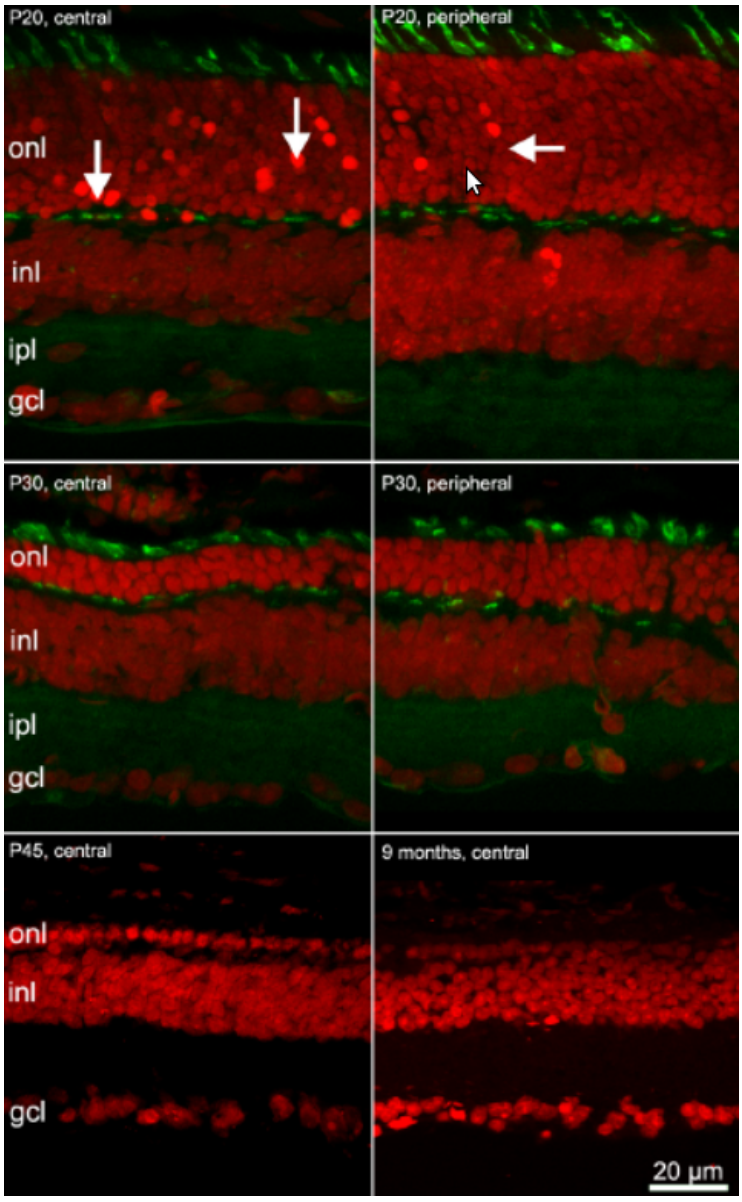

Figure 1.7: This image shows the progressive degeneration of photoreceptors. Red signal is obtained with ethidium nuclear staining; green signal represent the inner segment of cones and the synaptic endings in the OPL, obtained with PNA.

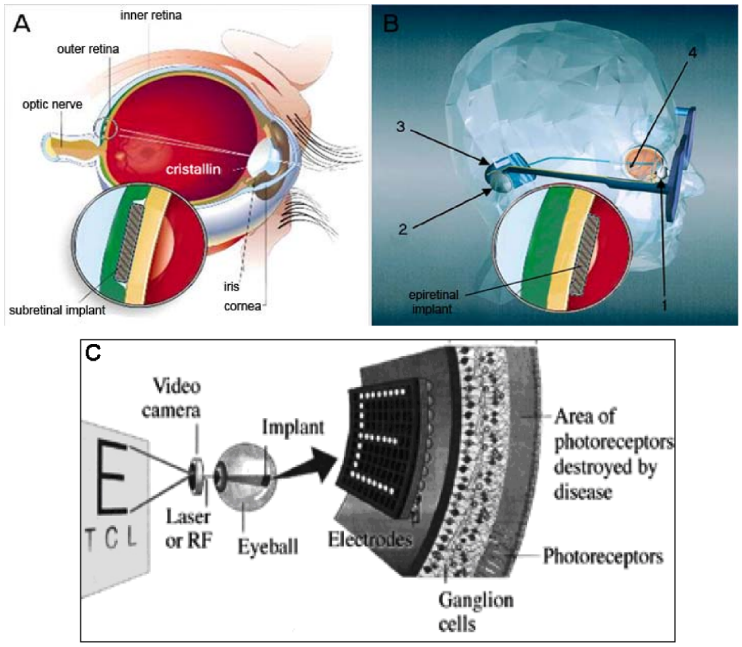

Figure 1.8: Schematic representations of subretinal (A) and epiretinal electronic implants (B): 1, camcorder mounted in a glass frame; 2, wireless transmitter; 3, extraocular junction box; 4, intraocular implants. In (C) is shown a simplified scheme of electronic epiretinal implants. From http://current.ucsc.edu/04-05/10-18/retina.asp.

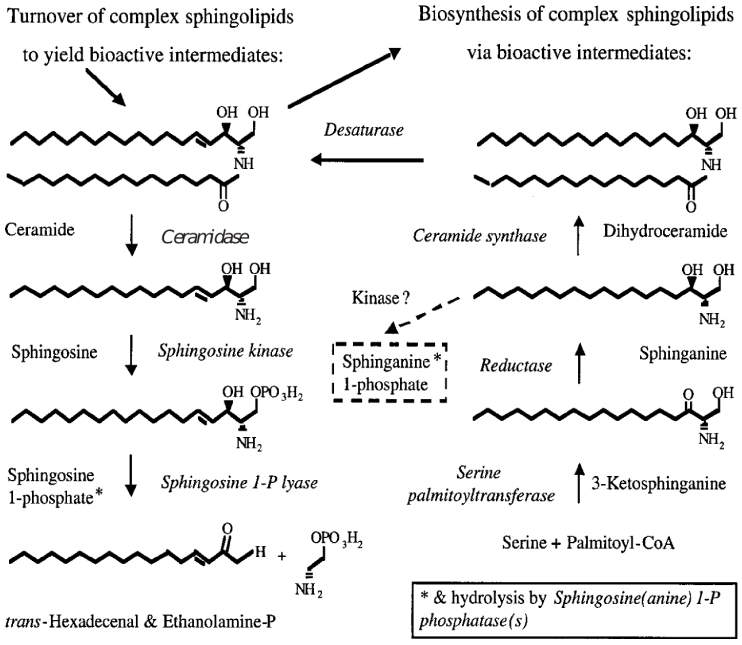

Figure 1.9: Biosynthetic and catabolic reactions for formation and removal of the major bioactive backbones of sphingolipids.

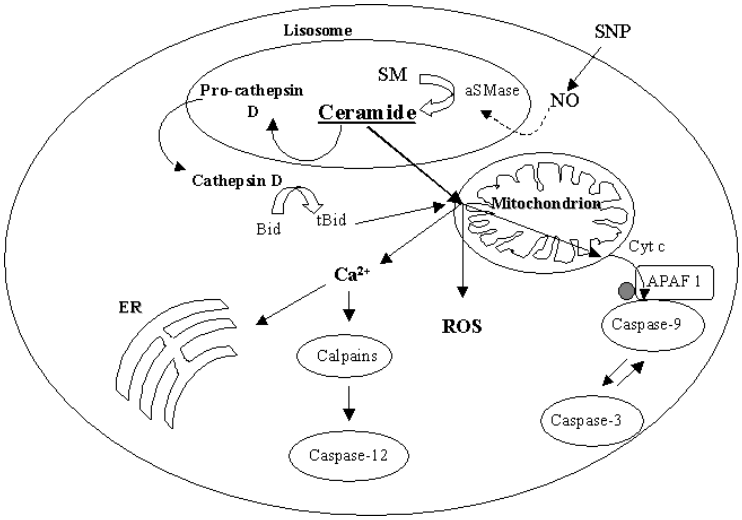

Figure 1.10: Schematic representation of the events that ceramide leads in cells for the activation of the mitochondrial apoptotic pathway.

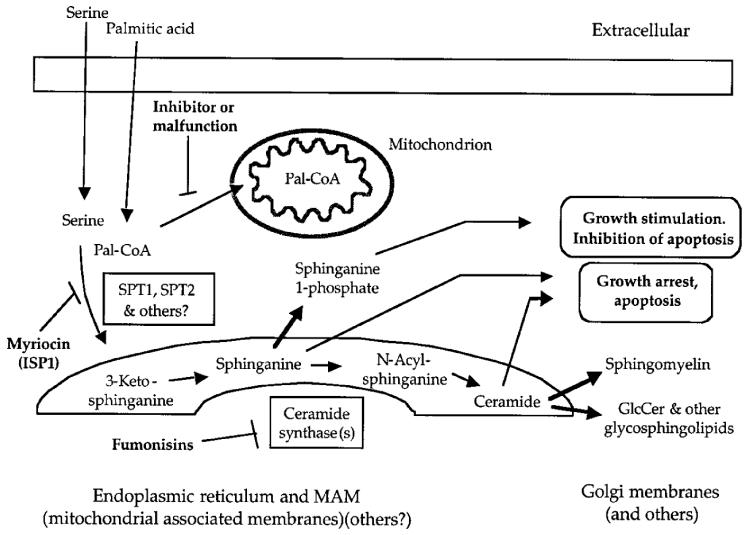

Figure 1.11: SPT1 and SPT2 are the two components of SPT. The sites of action of commonly used inhibitors (myriocin and fumonisin) are also shown. The subcellular locations of these reactions are indicated only for a general context; there are likely to be other sites where some of these reactions occurs. GlcCer, glucosyl-ceramide; Pal-CoA, palmitoyl-CoA.

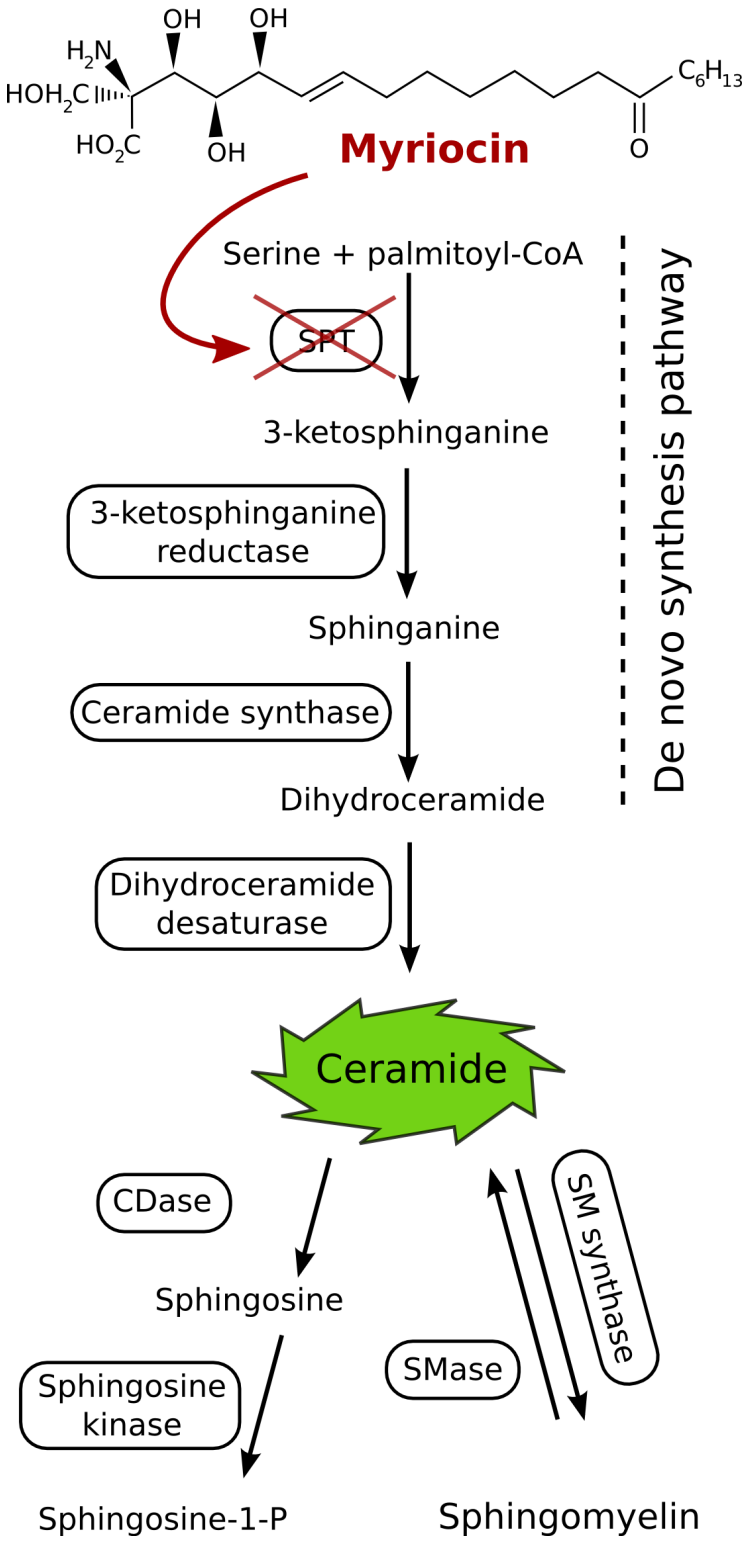

Figure 1.12: Schematic representation of the de-novo biosynthesis of ceramide and role of SPT. The chemical structure of Myriocin, an inhibitor of SPT is illustrated in this figure.

Chapter 2

Materials and Methods

2.1 Animals

All the experimental procedures involving animals were carried out according to the Italian and European guidelines for animal care (d.l. 116/92; 86/609/CE). Animals were maintained under a 12:12h light:dark cycle. Species and strains involved in this work include: rd10 mice (Jackson Laboratories strain B6.CXB1-*Pde6b*rd10/J) ([14]) and wild-type mice (Jackson Laboratories stain C57BL/6J).

2.2 Drug Delivery

The animals were treated with Myriocin, a known inhibitor of serine-palmitoil-transferase (SPT) which is the rate-limiting factor in Ceramide de-novo synthesis.

2.2.1 Acute Treatment: Intravitreal Injections

The acute treatment was obtained by means of intravitreal injections of Myriocin. Rd10 mice, aged P19, were anesthetized by intraperitoneal Avertin (0.5 g/ml 2,2,2-tribromoethanol in ter-amylic alcohol; 20 μl/g body weight). Using a glass micropipette driven by an oil Hamilton syringe, 500 nl of the solution of Myriocin (188M, in DMSO) was injected in the vitreous body of the right eye under a dissecting microscope, while vehicle alone was injected in the left eye. Local antibiotics were administered to prevent infections.

2.2.2 Chronic Treatment

We performed the chronic treatment by using eye drops containing Solid Lipid Nanoparticles (SLNs). The animals were divided in two groups. The first one was treated with SLNs loaded with Myriocin, the second one was treated with SLNs unloaded.
The administration of the eye drops started at P14 (the day when the animal first opens the eyes) and ended at the different ages of the animals (P21, P24, P27, P30, P35, P45, etc..). Eye drops were administered to each animal twice a

day. Each administration consisted in 0.5μl for the range P14-21, and in 0.75μl after P21.

2.2.3 Solid Lipid Nanoparticles

Solid Lipid Nanoparticles were pure lipid particles with a diameter of 40-200 nm containing a fatty acid core wrapped in a layer of phospholipids. For feasibility testing, SLNs were loaded with the fluorescent dyes coumarin (Across Organics), Nile red (Sigma-Aldrich), or N-(7-nitro-2-1,3-benzox-adiazol-4-yl)-1,2-dipalmitoyl-sn-glycero-3-phosphoethanolamine (NBD-DPPE; NOF Corporation) at a concentration of 0.01-0.02% (wt/wt). For experimental testing, SLNs were loaded with 0.15% (wt/wt) myriocin (Sigma-Aldrich). Briefly, an oil phase composed of melted stearic acid and Epikuron 200 (96% phosphatidilcholine; Cargill) and a water phase consisting of taurocholic acid sodium salt (Prodotti Chimici Alimentari) and water were combined in a warm microemulsion. Butylated hydroxyanisole and D,L-α-tocopherol were included to prevent oxidation.
The microemulsion was dispersed in cold water, resulting in the solidification of nanodrops which were then washed by tangential filtration (Amicon 8010 stirred ultrafiltration cell; Millipore). SLNs preparations were sterilized by filtration through a 0.2 μm filter before use.

2.3 Immunohistochemistry

2.3.1 Slice preparation

Adult mice (age $\sim$ 2 months) were anesthetized with an i.p. injection of Avertine (15 mg/kg, Sigma-Aldrich). Eyes were enucleated and fixed by immersion in 4% paraformaldehyde for 15 min, eyecup was dissected and maintained in paraformaldehyde for 1 hour; washed in 0.1M phosphate-buffered saline (PBS, pH 7.4) and cryoprotected in scalar dilution (10, 20, 30%) of sucrose. Eyecups were then included in Tissue Tek Optimal Cutting Temperature (OCT) compound (Miles incorporated, Elkhart NL) and sectioned at $-20°C$ into a cryostat. Serial sections of $18\mu m$ in thickness were collected on glass slips coated with gelatin (Fluka Biochemika).

2.3.2 Immunoreaction

The number of apoptotic photoreceptors for retina was assessed by morphological methods on retinas from rd10 mice injected with Myriocin at P19 and harvested at P21 (17 animals). Eyes were enucleated and fixed in 4% paraformaldheyde in 0.1M phosphate buffer. Retinas were isolated and stained with 2μM ethidium homodimer, a fluorescent DNA-binding molecule. Whole mount retinal samples were inspected with a Leica TCS-SP confocal microscope. The outer nuclear layer, containing the nuclei of photoreceptors, was sampled at 500μm intervals along the 4 retinal meridians. Photoreceptor pycnotic nuclei, condensed as a consequence of apoptosis, were counted in each scanned field and the total number of pycnotic photoreceptors was calculated for each retina with the aid of an image analyser. After the functional analysis of mice treated with Myriocin-SLNs or unloaded-SLNs, eyes were removed, fixed for 1h in 4%

paraformaldehyde in 0.1M PBS (pH 7.4), crioprotected by infiltration with 30% sucrose in the same buffer and frozen at $-20°C$ on a cryostat stage (Leica). Vertical sections of 14 μm were cut, collected on glass microacope slides, and stained with ethidium homodimer 2 in order to estimate the number of surviving photoreceptors by counting the rows of nuclei in the outer nuclear layer on high-resulution images of vertical sections obtained from both central and peripheral retinal areas ([101]).
Photoreceptor morphology and retinal histology were studied by immunocytochemistry and confocal microscopy on retinal sections ([29]). Primary antibodies used were: anti-blu/red-green cone-opsins (rbbit polyclonal, 1:1000; Chemicon), anti-PSD95 (rabbit polyclonal, 1:500; Millipore), anti-PKC (mouse monoclonal, 1:100; Sigma Aldrich), anti-Goα (mouse monoclonal, 1:500; Sigma Aldrich). All of the primary antbodies were revealed with secondary antibodies anti-mouse or anti-rabbit conjugated with Alexa Fluo 488 or 568.

2.4 Western Blot Analysis

Cone-opsin proteins were assessed by semi-quantitative western blot, from both rd10 treated and untreated mice retinas, at different ages. 60 g of protein from each sample was electrophoresed on a 12% SDS-polyacrylamide gel. Proteins were transferred to PVDF (Immobilon-P Transfer membrane 0,45 μm, Millipore) membrane using transfer buffer (25mM Tris-HCl pH=8.3, 192mM glycine, 20 methanol). The protein blot was blocked by exposure to 3% non-fat dried milk and 0.1% NP-40 (Igepal, Sigma) in 20 mM Tris-HCl, 500mM NaCl (TBS) pH=8 at room temperature for 45 minutes. After the blocking procedure, the membrane was incubated overnight at $4°C$ with primary antibodies: rabbit polyclonal anti-blu cone-opsin or anti-R/G cone-opsin (1:200, Santa Cruz) diluited in blocking buffer. The reactions were revealed with HRP-conjugated secondary antibodies (anti-rabbit IgG, 1:10000, Chemicon), incubated for 2 hours at room temperature. Bands were visualized using a chemiluminescence kit (ECL western blotting detections agents, Amersham Biosciences, UK) and quantified by optical density. On the same blots, cone-opsins content, were normalized to the amounts of β-actin. The PVDF membrane was incubated in stripping buffer (glycine 0,1M pH 2.5) for 5 minutes. Then the membrane was washed in TBS for 6x10 minutes at room temperature. The protein blot was exposed to the blocking medium at room temperature for 45 minutes. After, the membrane was incubated overnight at 4C with the mouse monoclonal anti-βactin (1:2000, Sigma) in blocking buffer. The reaction were visualized with HRP-conjugated secondary antibodies (anti-mouse, 1:10000) for 2 hours at room temperature.

2.5 Biochemical quantification of retinal ceramide

Basic ceramide (CER) values were assessed biochemically on retinal extracts from rd10 and wt mice aged P14, P22 and P30 (n=6 each group). Animals were anesthetized as above, their eyes quickly removed and the retinas isolated in oxygenated ACSF medium, then frozen on dry ice for lipid extraction. Briefly, 30 nmol of lipids, quantified as inorganic phosphate, were incubated in

the presence of 20 μl β-octylglucoside/dioleoylphosphstidilglycerol micelles, 2 mM dithiothreitol, 6 μg of Escherichia Coli DGK (Calbiochem), 1 mM ATP, 1.3 Ci of [y32 -P] ATP (3 Ci/mol) in a final volume of 100 l at 25C for 45 minutes. Radioactive lipids were separated, along with reference lipid standards, by thin layer chromatography (TLC), with chloroform/methanol/acetic acid/water (10/4/3/2/1, by vol). Endogenous CER content was determined by the DGK assay ([91]). Radioactive CER phosphate spots were visualized by autoradiography, scraped and counted by liquid scintillation CER values of different animals were averaged and referred to total phospholipids. CER was quantified also from retinas of mice after intraocular injections of Myriocin as described above. Left and right retinas of each animal (n=16) were isolated at P21 and processed separately for CER biochemical assay.

2.6 Electroretinogram

2.6.1 Animal preparation

Animals were dark adapted overnight before the experimental session, mice were anesthetized with an i.p. injection of ketamine (2.5μg/g body weight) and xylazine (0.3μl/g body weight). A single injection was sufficient to maintain the subject deeply anesthetized for the whole experimental session (3 to 4 hours), as verified by the absence of corneal reflexes. Pupils were dilated with drops of 1% tropicamide (rats) or 1% atropine (mouse) (both from Sigma-Aldrich), while constant body temperature of $\sim 37°C$ was maintained by an electric thermal blanket placed beneath the animal. A gold, ring-shaped recording electrode was placed over each cornea, a thin layer of methylcellulose (Lacrinorm, Farmigea Pisa) allowed the cornea to remain moist throughout the experiment. A needle electrode inserted in the rear portion of the neck was used for ground signalling in mice. ERG signals were amplified by a 1000x factor and filtered in the frequency range of 0.3 - 500 Hz by a PC board amplifier (LACE elettronica, Roma Italy), digitized at 12.8 kHz by a 16-bit DAQ board (model PCI-MIO-16E4) driven by a custom made LabView 6.1 software (both from National Instruments, Austin TX).

2.6.2 Light stimulation

Light stimulation protocols were generated by a 16-bit PC DAQ interface (PCI-MIO-16E4, National Instruments, Austin TX), voltage-encoded signals were converted into light intensity variations by a device developed in our laboratory, described in [21]. Light stimuli were delivered into a Ganzfeld sphere of 30 cm in diameter, with internal surface coated with highly reflective white paint, in order to ensure an uniform illumination over the whole retinal surface.
For the flash stimulation protocol, an electronic flash unit (Sunpak B3600 DX , Tocad Ltd. Tokyo JP) delivered flashes of white light, whose energy decayed with a $\tau = 1.7$ ms and whose scotopic efficacy was estimated following [59]. The estimated retinal illuminance was 5.7×10^5 Φ (Photoisomerization per rod) per flash. The whole spectrum of light intensities were achieved by placing optical neutral density filters within the light path. The luminance was expressed as a

function of time by the equation(2.1):

$$\begin{aligned} L_{(t)} &= L_0\,(1 + m \cdot sin\,(\omega t)) \\ &= L_0\,(1 + m \cdot sin\,(2\pi\nu t)) \end{aligned} \tag{2.1}$$

where: L_0 is the mean luminance, estimated to be $\sim 40\ \phi$; m is the contrast value, allowed to assume values from 0 to 1, a constant value of 0.85 was used during all the experiments; ν is the frequency of the generated sinusoid, varying from 0.3 Hz to 30 Hz within each trial.
Estimations of light intensity impinging on the rodent retina were carried out according to [58] using the equations (2.2) (2.3).

$$F_{(\lambda)} = \frac{I}{E_{photon}} = \frac{I}{h \cdot \frac{c}{\lambda}} \tag{2.2}$$

where: $F_{(\lambda)}$ is the photon density $[photons\ m^{-2}\ s^{-1}]$; I is the measured irradiance $[W\ m^{-2}]$; h is the Planck constant $(6.6626 \times 10^{-34}\ J\ sec^{-1})$; c is the light's speed in a vacuum $(2.99792 \times 10^{8}\ m\ s^{-1})$ and λ is the wavelength of the light [m].

$$\frac{\Phi}{\Delta t} = F_{(\lambda)} \cdot \tau_{(\lambda)} \cdot a_{c(\lambda)} \cdot \frac{S_{pupil}}{S_{retina}} \tag{2.3}$$

where: $\frac{\Phi}{\Delta t}$ is the estimated photoisomerization per rod per second delivered to the retina; $F_{(\lambda)}$ is the photon density; $\tau_{(\lambda)}$ is the transmission of the pre-photoreceptor ocular media (estimated as 0.7 for both rats and mice); $a_{c(\lambda)}$ is the "end-on collecting area" of rod photoreceptors (1.3 μm^2 for rats, 0.87 μm^2 for mice); S_{pupil} is the area of the fully dilated pupil (7.1 μm^2 for rats, 3.2 μm^2 for mice); S_{retina} is the area of the retinal tissue (55 μm^2 for rats, 18 μm^2 for mice).

2.6.3 ERG protocols

Mice were subjected at two different ERG protocols: scotopic and photopic ERG. The responses to the brightest flashes, of the scotopic ERG, include mixed rod and cone components patway, whereas in photopic ERG the response generate only from the cone patway. In scotopic ERG, mice were subjected to six different flash intensities, each repeated five times, with an interstimulus interval that ranged from 60s for dim light to 5 min for the brightest flashes. Five ERG traces at each flash luminance were averaged before measurements of a- and b-wave amplitudes. The amplitude of the a-wave was taken as the different between baseline and the lowest value, whereas the amplitude of the b-wave was measured from the trough of the a-wave to the peak of the b-wave.
Isolated cone components were obtained by superimposing test flashes on a background of saturating intensity for rods (30 cd*s/m2).
From the ERG responses obtained by photopic stimulation we analyser the Oscillatory Potentials (OPs) ([52], [114]). OPs are specific components of electroretinograms and consist of a series of wavelets embedded in the ascending limb of the ERG b-wave. Analyze the OPs is a method in order to understand the functionality of the inner retina, in fact OPs are generated from the inner retina, presumably amacrine cells and adjacent retinal neuron network ([106]).

Chapter 3

Results

3.1 Retinal content of Ceramide

To evaluate if, in the rd10 mouse, there are altered levels of retinal ceramide, retinas were obtained from both rd10 and wt pups between P12 and P30. Total retinal ceramide, normalized to the amount of inorganic phospate (Pi) from total phospholipid, was similar in the two grups until P16; A P21, time of peak of rods degeneration, the levels of ceramide was significantly increased in rd10 retinas respect to wt retinas (3.1). Note that after P16 in rd10 retinas the levels of ceramide increase while in wt retinas the ceramide content starts to decrease.

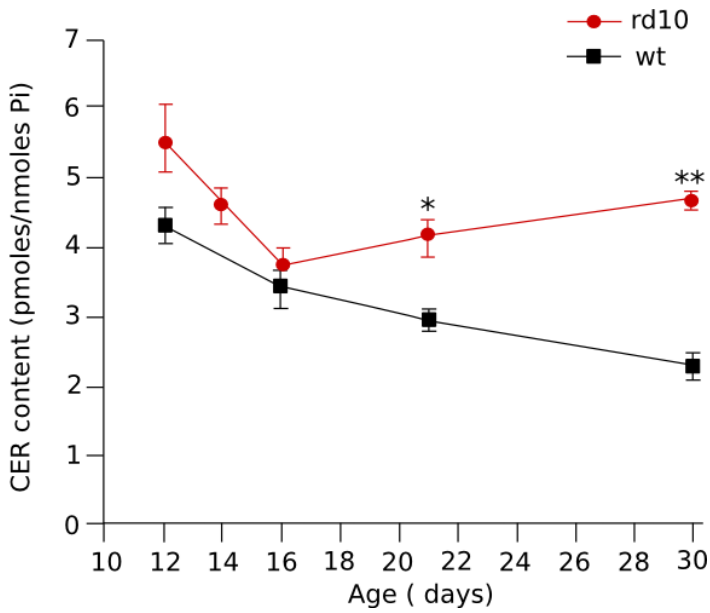

Figure 3.1: Time course of endogenous ceramide content in retinas of littermaters during the first month of life: in rd10 retinas a significantly increase of the ceramide levels is in concomitance with the peak of retinal degeneration (* P=0.05 t test;** P=0.001 t test)

3.2 Pharmacological effects on Retinal Ceramide levels and rod-photoreceptors survival

3.2.1 Acute Treatment

In order to evaluate whether the high levels of ceramide in phatological conditions were reduced by a pharmacological treatment, we administered Myriocin, an inhibitor of the biosynthesis of ceramide. Miryocin was administered by intraocular injection on P19 mice followed by ceramide quantification on P21. Myriocin injection into the right vitreous body reduced the retinal ceramide levels with respect to the left eye which was injected with the vehicle alone. The results show that this treatment was effective in bringing ceramide to levels considered normal for P21 mice (3.2).

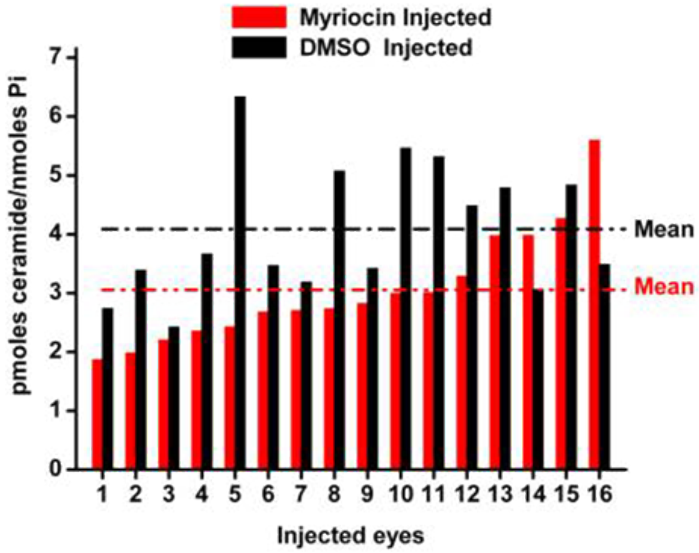

Figure 3.2: Effect of intraocular injection of Myriocin on retinal ceramide content in rd10 mice. In 14 of 16 animals, Myriocin lowered ceramide content; Myriocin induced a 25.4% reduction in mean ceramide content, from 4.09 pmol/nmol Pi to 3.05 pmol/nmol Pi (SD=0.97) (P=0.011, paired t test)

The protective effect of a single injection of Myriocin on photoreceptors survival was investigated by both counting the number of apoptotic photoreceptors and recording the scotopic ERG, in retinas from treated and untreated-eyes. Isolated retinas were stained with a fluorescent nuclear dye to identify pycnotic nuclei (condensed DNA, cell start to die by apoptotic process) and visualized by confocal microscopy. Retinas from treated-eyes had fewer intensely stained nuclei than untreated-eyes (3.3). Qunatitative analysis shows that a single injection of Myriocin was effective in reduced the number of pycnotic photoreceptors (reduced by 52.6%).
The scotopic ERG was recorded from P21 animals after two days after injection the treatment with injection of myriocin (right eye) and vehicle alone (left eye). The scotopic ERG response to flashes of light of different intensities was

measured in dark adapted animals (3.4). Surprisingly, no significant difference could be detected in the ERGs of eyes injected with myriocin (red bar) or with the DMSO vehicle (black bar) (3.5).

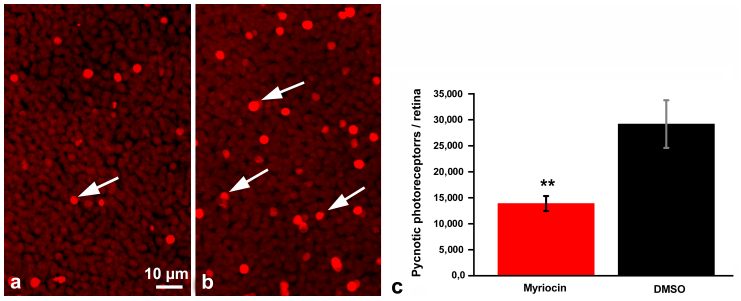

Figure 3.3: Fluorescence microscopy of retina whole mount after a single injection of Myriocin. Retinas, from myriocin treated eye (A) and vehicle treated eye (B), were fixed and stained with ethidium homodimer. Quantification of pycnotic nuclei (C), myriocin injection was associated with a reduction in the number of pycnotic photoreceptor nuclei on P21 (** P=0.007, t test)

In order to evaluate if a single injection of myriocin was not sufficient to induce a recovery in retinal fuctional we performed a chronic treatment with myriocin.

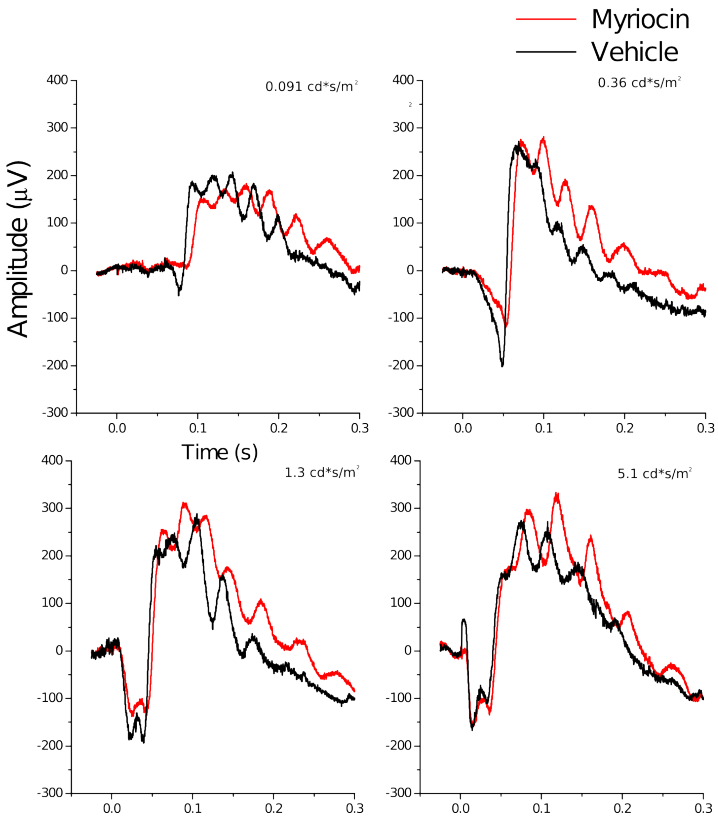

Figure 3.4: Example of ERG responses at different intensity of light. The red tracks represent the treated eye with myriocin and the black tacks represent the treated eye with DMSO (vehicle). A single intraocular injection of Myriocin did not have significant protective effects on retinal function, as shown by similar amplitudes and kinetics of a and b-waves in the two experimental conditions

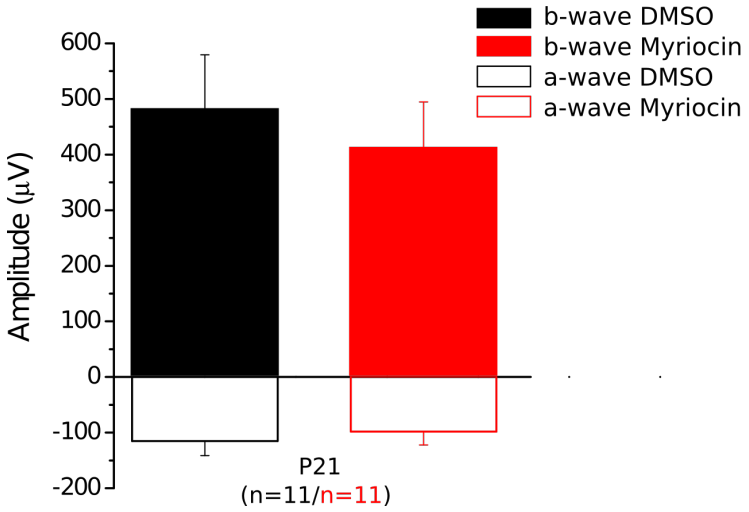

Figure 3.5: Average of eleven treated and untreated eyes. Treatment with a single injection with myriocin didn't induce significant change in both a-wave and b-wave

3.2.2 Chronic Treatment

The first chronic treatment was performed by instilling, once daily, eye drops of a solution of myriocin (1μl of 3.77 mM solution in DMSO) to the cornea of rd0 mice once daily for 4 days. Microscopic analysis for pycnotic nuclei and ceramide quentification revealed no significant difference between myriocin- and DMSO-treated eyes, suggesting that possibly the drug could not cross the external tissue of the eye thus failing to reach the retinal terget.
We therefore turned to a different strategy, based on the use of solid lipid nanoparticles (SLNs), that could enable the drug to diffuse across the ocular tissue. We first investigated whether SLNs pure lipid particles with a diameter of 40-200nm labeled with a fluorescent dye, instilled into the conjuntival sac, could reach the retinal layers ([101]) in wt mice and showed by confocal microscopy the presence of bright aggregates in the outer nuclear layer (ONL) and also between photoreceptors and retinal pigment epithelium ([101]).
SLNs were subsequently loaded with myriocin. The concentration of the drug in different preparations was between 0,4 and 1.0 mM.
First of all, a eye drop solution containing the Myriocin-SLNs was administered to wt mice starting on P14 upto P24. Wt mice included two distinct groups: treated (Myr-SLNs) and control (Vehicle-SLNs) groups. After the treatment sample of retinas from treated mice were collected to evaluate by morphological analysis ([101]), possible adverse effects onthe retinal structure. Other animals from same group were used to evauate the functional performance of the retina by measuring the ERG response (3.6). Subsequently we turned to the treatment with myriocin of rd10 mice. The protocol of the daily eye drop treatment of transgenic mice sterted on P14 to end at different ages (P21, P24, P30, P35) in various animal groups. From P21 to P35, different animals underwent ERG testing of retinal function followed by retinal microscopic analysis (3.7). In both control and myriocin-treated rd10 mice, mean aplitude of the b-waves and a-waves decreased progressively over time in concomitance with retinal degeneration. However, the b-wave amplitude of myriocin treated animals was substantially higher than that recorded from control animals at all time execept P35. Significant diffrences were observed, between the two groups, in the amplitude of a-wave at P30 and P35 (3.8).
Also, microscopic analysis of vertical section of treated and untreaed retinas, revealed a protective effect of myriocin on the number of photoreceptor rows (3.9); further, the morphology of surviving photoreceptors was preserved as well as dentrites in rod bipolar cell ([101]).

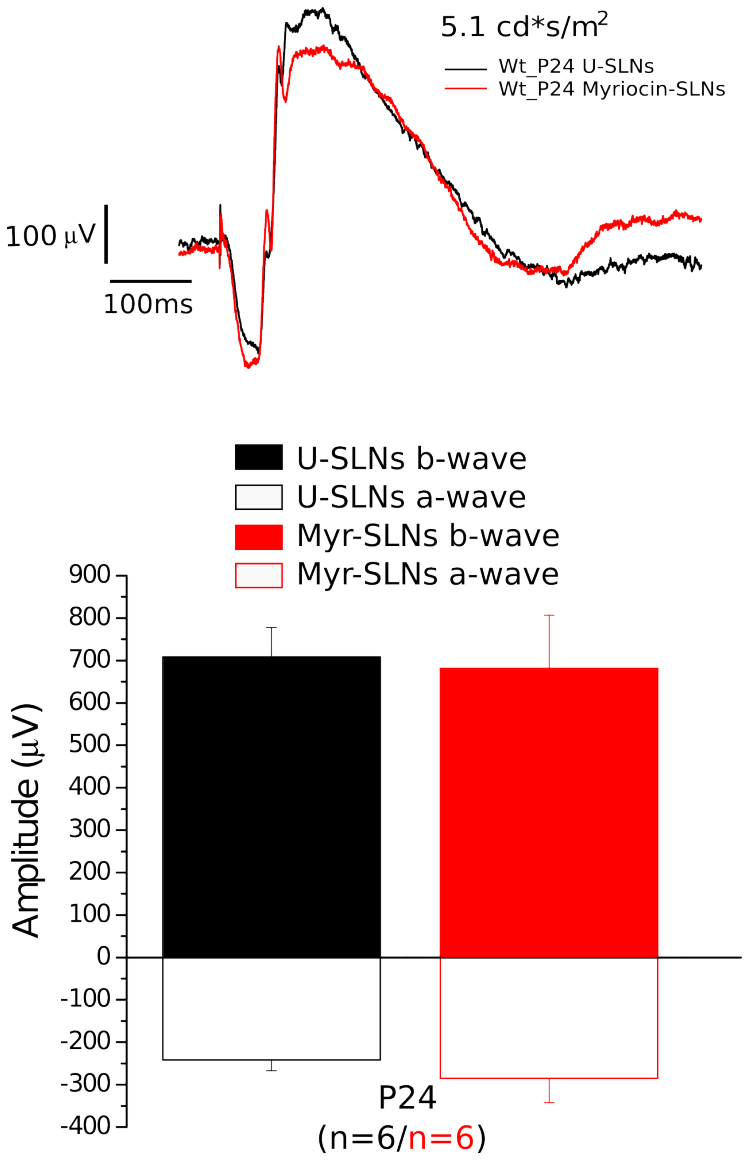

Figure 3.6: Lack of functional effects of myriocin on wild-type mouse retinas. The upper panel represents ERG traces obtained from a wild type mouse after prolonged administration of myriocin-SLNs. The bottom panel is the average of six treated and untreated mice. Treatment with myriocin didn't induce significant changes in both a-wave and b-wave amplitudes

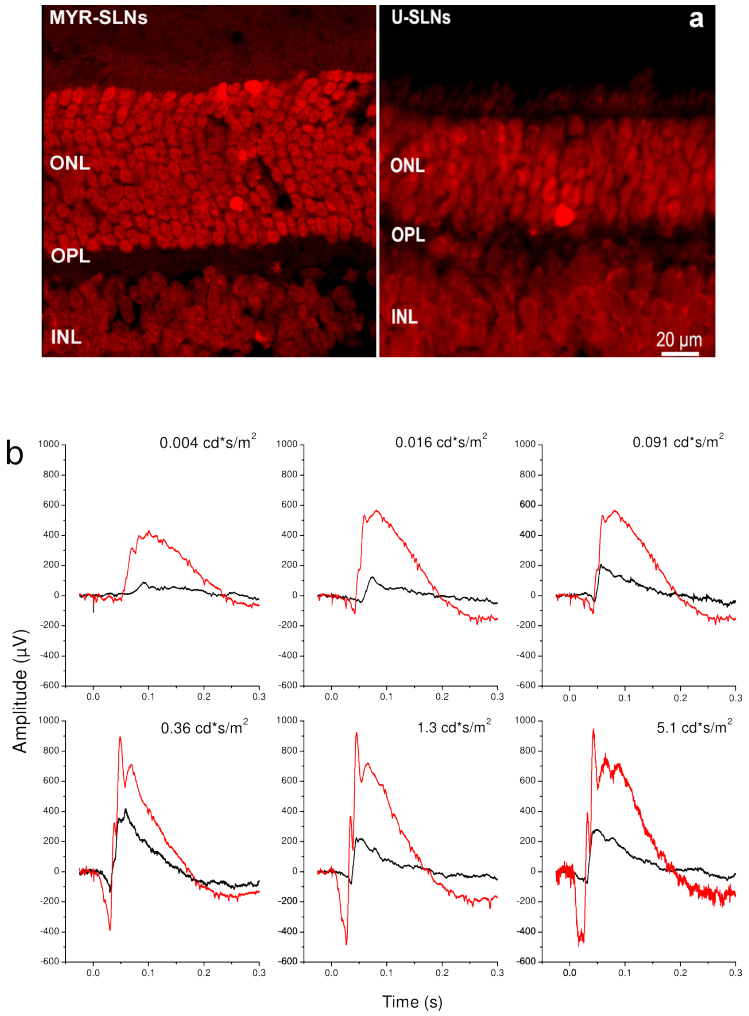

Figure 3.7: Morphological and functional effects in the P24 rd10 retinas after chronic treatment with Myriocin-SLNs. (A) Confocal analysis of treated and untreated rd10 mice. The number of photoreceptor rows was increas in Myriocin-SLNs retinas respect to vehicle-SLNs one. (B) ERG responses obtained from the same animals at different intensity of flashes light

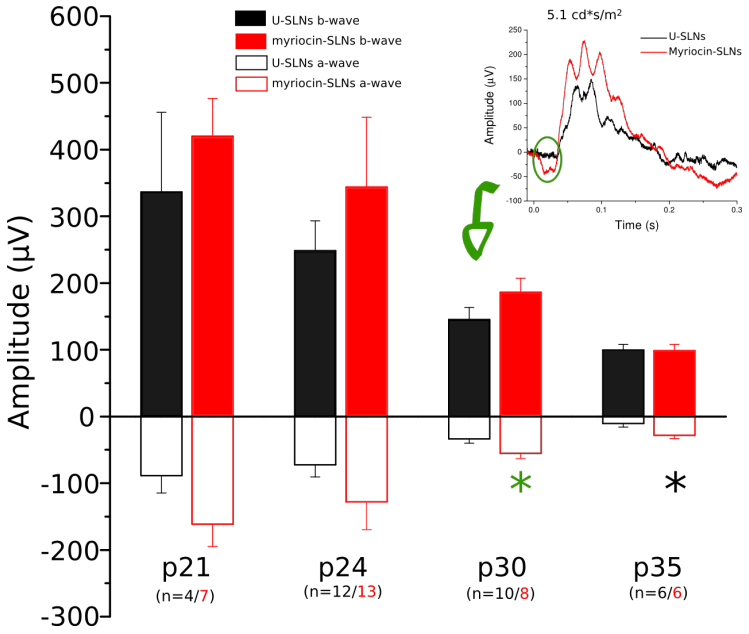

Figure 3.8: Amplitude of ERG a and b-waves from eyes of rd10 mice treated with control SLNs or myriocin SLNs from P14 and exposed to light flash of 5.1 cd*s/m2. The insert represents an example of ERG recording at P30.

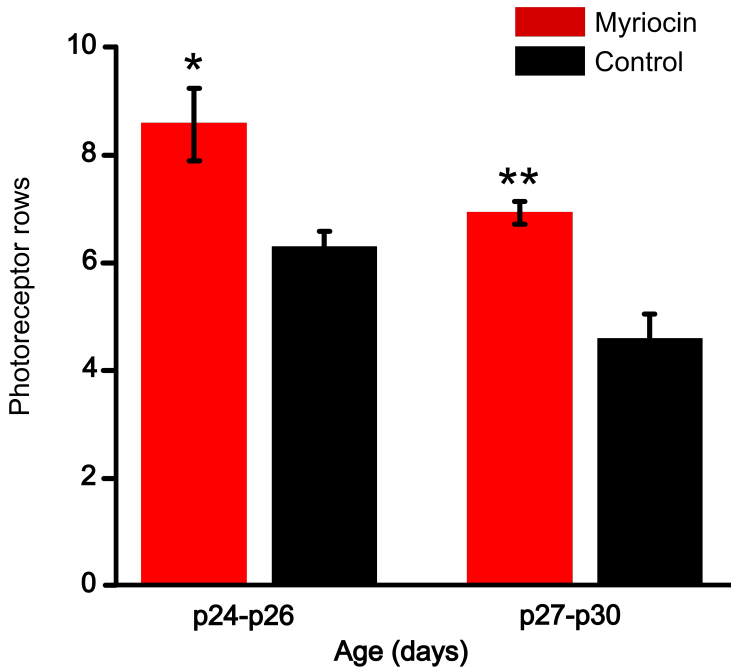

Figure 3.9: Quantification of photoreceptor rows at P24 and P30 in the rd10 mice treated with control SLNs or myriocin-SLNs (* P=0.002, ** P=0.003 *t* test)

3.3 Morphological and functional evaluation of the retina in the later stages of RP in rd10 mice

RP is mainly caused by mutations in rod-photoreceptors specific genes, but in the later stages also cone-photoreceptors, whose genes are not affected, start to die. In this study we analyzed the cone photoreceptors functional status respect to wt mice. We used scotopic and photopic ERG in rd10 mice aged P20. At this stage of the animal life only the rod-photoreceptors are facing the apoptosis process that leads to their eventual loss. It seems therefore reasonable to assume that cones functional performance were similar to that of wt. The results illustrated in (3.10 A) confirm the prediction that the rod-driven ERG response amplitude is smaller in the rd10 P20 mice than in wt ([29]) and that both response amplitude and sensitivity of the cone pathway in rd10 and wt mice is similar 3.10 B.
Further, analysis of the kinetics if the ERG response reported in figure 3.11 shows that responses from both rods and cones are significantly slower in rd10 that in wt mice([29]). This result indicates that in the early stages of RP, also cone photoreceptors reveal symptoms of functional damage(3.11).
It is well known that in RP patients the residual vision is based on cones that survive longer than rods, but with time also cones are doomed to death. The present results show that despite a longer survival also cones show signs of damage at already early stages of retinal degeneration.

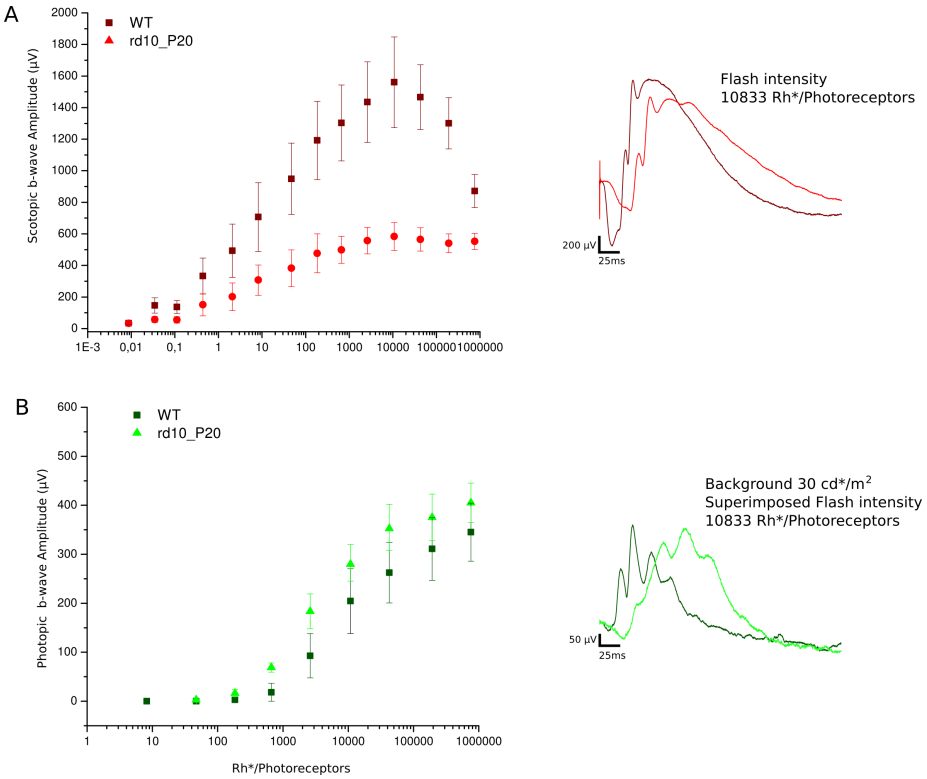

Figure 3.10: In this figure the red plot represents the response obtained mainly from rod patway and the green plot represents the ERG responses obtained from cone patway

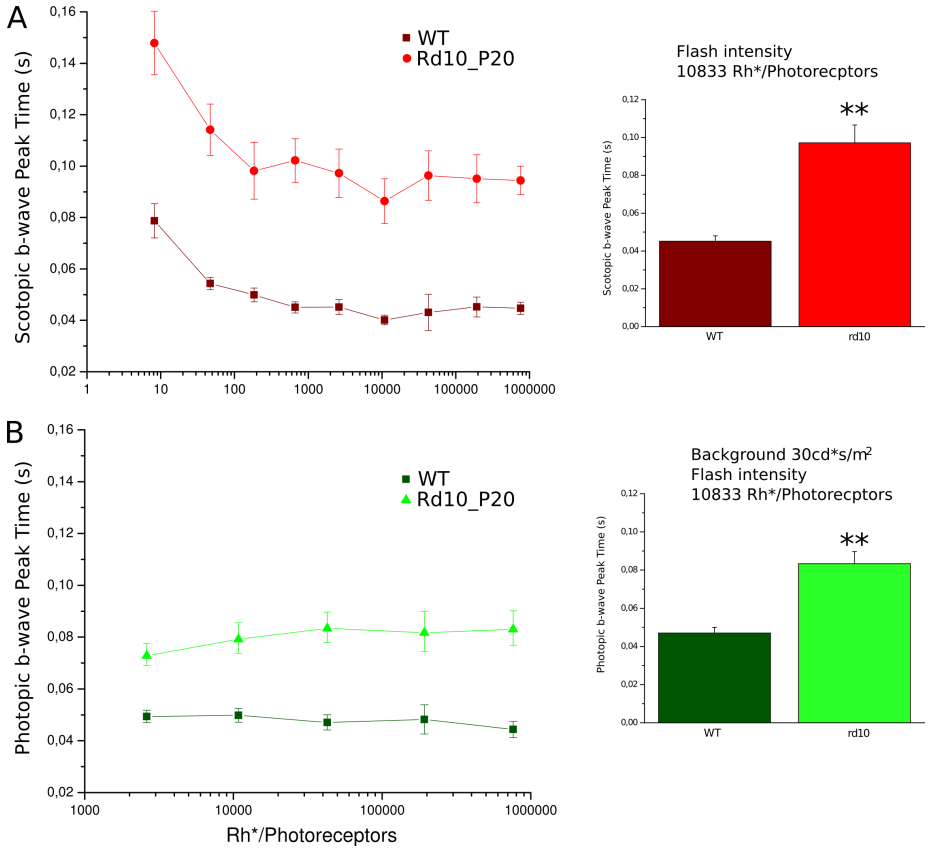

Figure 3.11: Peak time obtained from rod patway (red) and cone patway (green). Note that in both panels the peak of the responses in rd10 mice is slower than wt mice (** P=0.002 t test)

3.3.1 Time-course of cone-photoreceptors function in rd10 mice

In order to evaluate the cone-photoreceptors function we measured photopic-ERG in rd10 mice at different ages (3.12). Animals were light-adapted with a steady background wich saturated the rod-photoreceptors, after that a bright flash stimulated the cone responses. The cone b-wave amplitude in rd10 mice at P20 was about 279.6 μV (SD 40.2 μV) (3.12 B). This result shows that, in the early stages of RP, as far as the response amplitude is considered, cone-photoreceptors produce seemingly normal responses to light. Furthermore, as shown in fig. 3.12 (A) also the light sensitivity of cone-photoreceptors in rd10 P20 mice was normal. However, starting from P30 both sensibility and amplitude of rd10 mice started to decrease (3.12). By the time, cone-photoreceptors start to die, rods are nearly copletely lost. A massive loss of function of the cone-photoreceptor at around starts P40.

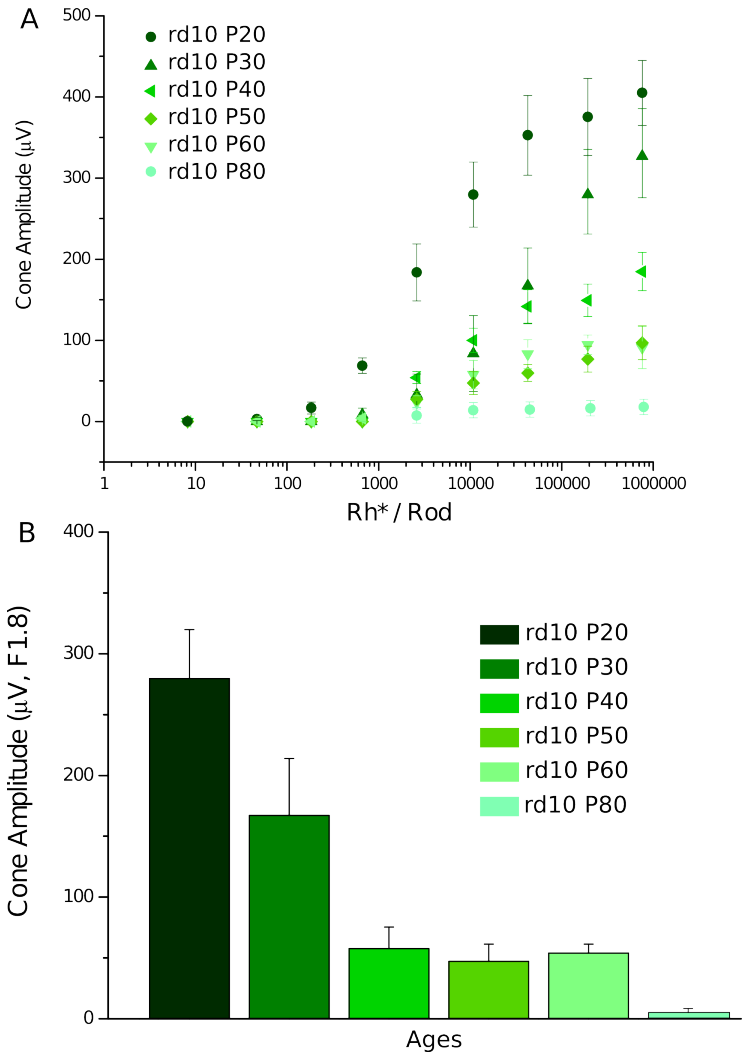

Figure 3.12: (A) Average of b-wave amplitude at different intensity of flash light superimposed on steady background. (B) Time-course of the cone-photoreceptors activity in rd10 mice. In the early stages of the patology the cone b-wave in rd10 was the same of wt mice; On P30 the cone b-wave starts to decrease and from P40 up to P60 the amplitude of b-wave was stably lowered

3.3.2 Myriocin effects on cone-photoreceptors survival

There is a large consensus on the notion that death of cones is a consequence of the loss of rods ([71], [89]). Up to now, however, no evidence is available to explain the process that may cause of the secondary degeneration of cones. Regardless of the mechanism that causes the death of cones, following the rod loss it seems reasonable to predict that prolonging the rods survival by reducing the levels of ceramide may prove beneficial also to cones. The rationale for this proposition may be dual: a) the hypothesized dependence of cone survival from the rod integrity, b) a direct effect on cone of the reduced levels of an apoptotic agent. These possibilities were then tested by analyzing the effects of Myriocin chronic treatment on fuctional, biochemical and morphological tests of cone photoreceptor cells integrity.
In this study the treatment of rd10 mice started at P14 and extended up to P20, P30, P40, P50 and P60 respectively. Cone ERG response amplitude and kinetics, (3.13, 3.14) as well as sensitivity were shown to improve following chronic treatmen with myriocin at P40 and P60. The effects of myriocin treatment was also confirmed by western blot analysis for cone-opsin protein (3.15).

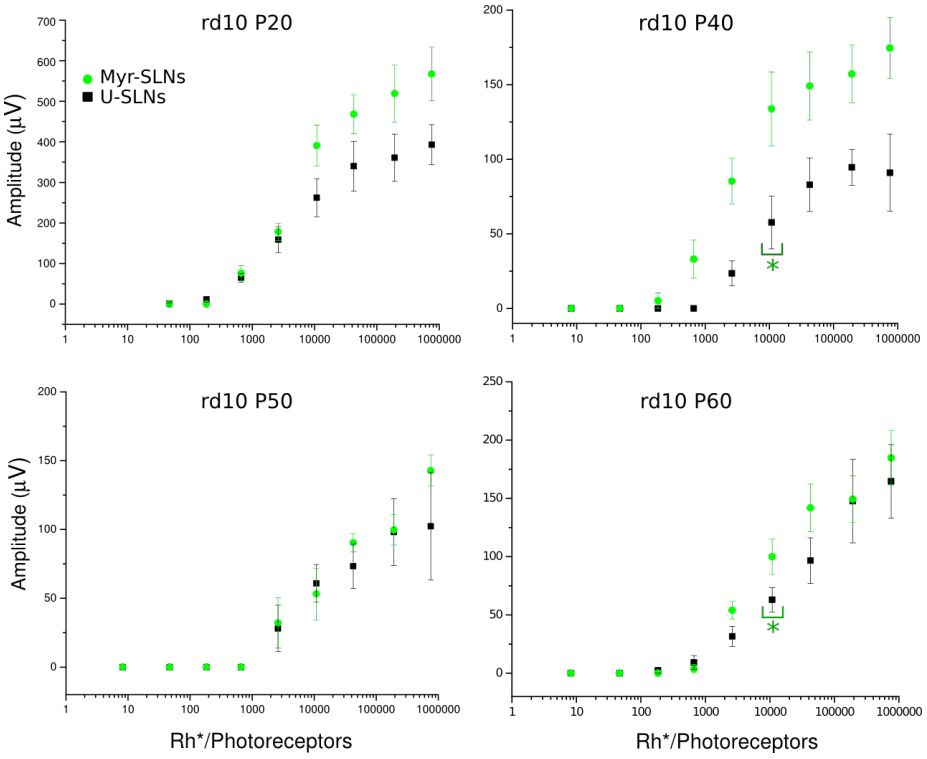

Figure 3.13: Photopic ERG recording from rd10 mice at different ages. The green plot represents the responses of the animals groups treated with Myriocin-SLNs, the black plot represents the responses from animal groups treated with vehicle-SLNs. The improvement of the cone b-wave amplitude was significantly on P40 and P60 rd10 mice

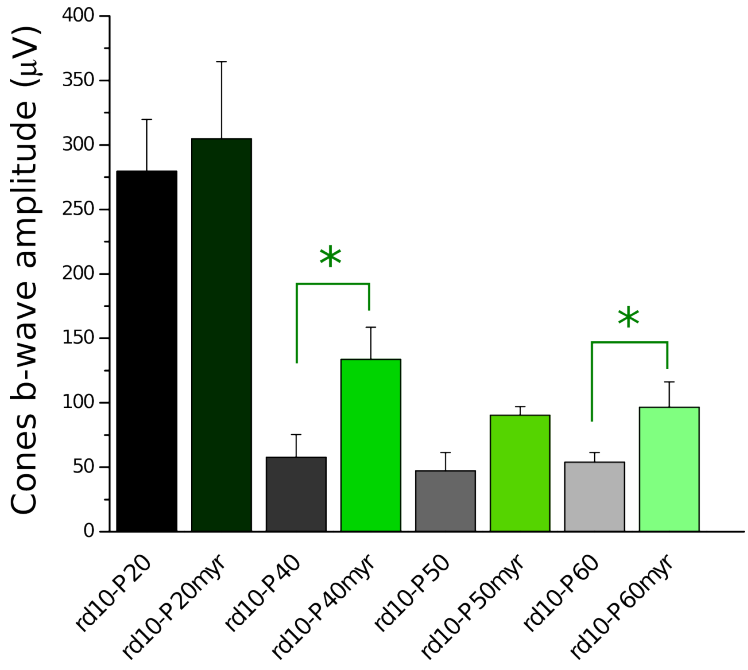

Figure 3.14: Average of b-wave amplitude from cone-photoreceptors patway. Bars in gray scale represents groups treated with vehicle-SLNs, while bars in green scale represents groups treated with Myriocin-SLNs. The treatment with myriocin tends to improve the cones features at each time point; at P40 and P60 the cones b-wave amplitude was significantly increased (* P=0.05 *t* test) in myriocin treated animals respect to control animals

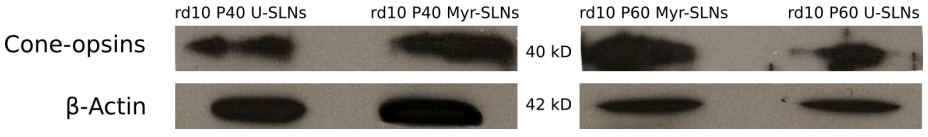

Figure 3.15: Western Blot analysis performed after myriocin treatment. For the semi-quantitative western blot analysis, the four lines were loaded with retinal homogenates (60μg of total protein); cone-opsin content in the myriocin-SLNs treated retinas was higher than vehicle-SLNs treated retinas

In order to understanding the status of the photoreceptors synapses to bipolar cells, we analyzed the morphological feature by using confocal microscopy (3.16, 3.17, 3.18). The confocal microscopy analysis showed that in the myriocin treated retinas the layer structure was more conserved than in untreated retinas. In rd10 P40 treated retinas the status of retinal layers were improve respect to untreated retinas (fig. 3.16). In fig. 3.17 the red staining represents the PKC protein, a specific marker for the rod-bipolar cells; green staining represents the PSD95 protein, a specific marker for both rod and cone pre-synaptic terminals. This image shows that in myriocin-treated retinas, the dendritic terminals were present in corrispondece to PSD95 while in vehicle treated retinas the bipolar cells were completely bare. This observation suggests that in myrocin treated retinas the synaptic connectivity is maintained. Possibily, prolonging the survival of photoreceptors facilitates the formations of ectopic synapses from cone-photoreceptors to rod-bipolar cells ([87]). Further, fig. 3.18 shows that, also in retinas from rd10 P60 mice, cone-photoreceptors are most intact in treated mouse respect to untreated one.

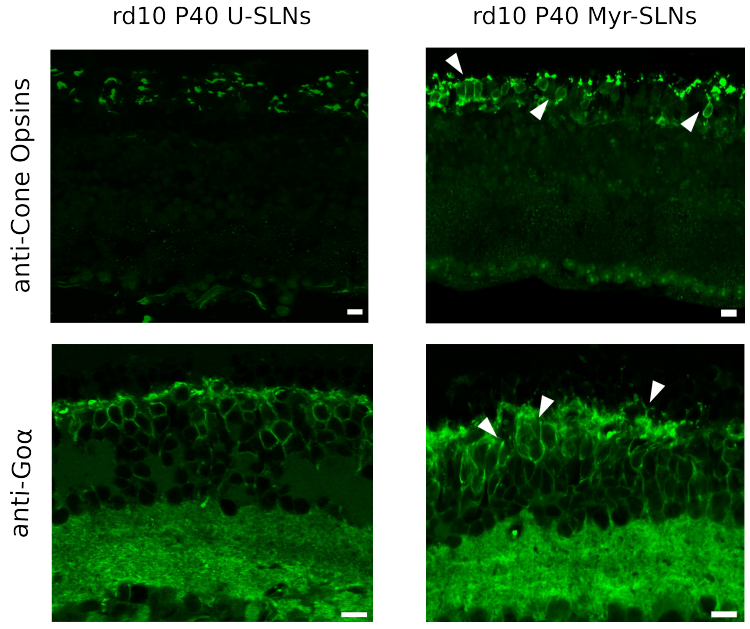

Figure 3.16: Confocal microscopy analysis from both treated and untreated retinas in P40 mice. The green staining, in the upper panels, was obtained with antibody anti-cone opsins blu and red/green while in bottom panels, the green staining was obtained with an antibody anti-Goα. In the upper myriocin-SLNs treated retinas the arrows indicates the inner segment, body cell and synaptic terminal of cone-photoreceptors; in bottom treated retina the arrows indicate the dendritic terminals and bodies of ON bipolar cells

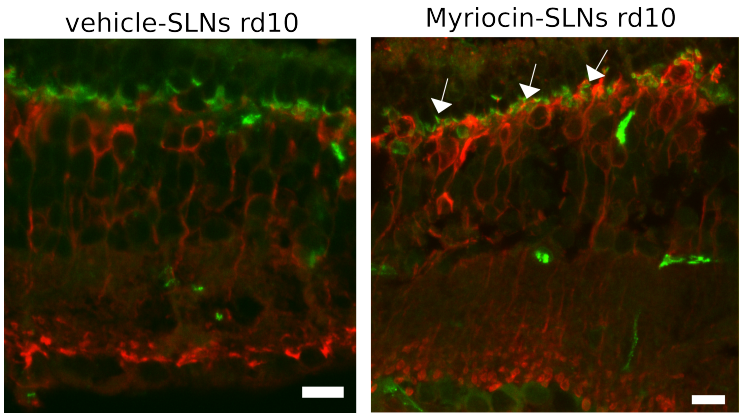

Figure 3.17: Confocal microscopy analysis from both treated and untreated retinas in P60 mice. The red staining was obtained with antibody anti-PKC and the green staining was obtained with antibody anti-PSD95. In the myriocin-SLNs treated retinas the arrows indicates the dendritic terminals

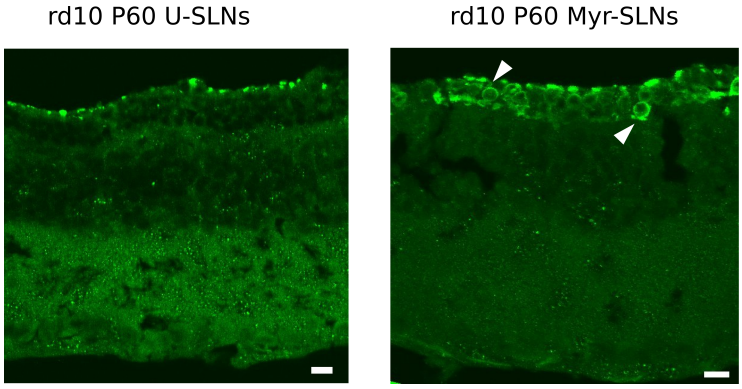

Figure 3.18: Confocal microscopy analysis from both treated and untreated retinas in P60 mice. The green staining was obtained with antibody anti-cone opsins blu and red/green. In the myriocin-SLNs treated retinas the arrows indicates the cone-photoreceptors

3.3.3 Myriocin effects on inner retina

Furthermore, we analyzed the Oscillatory Potentials (OPs) from the photopic ERG responses. The OPs are generated at the inner retinal mainly the amacrine cells. Amacrine cells have animportant role in retinal processing eithin the inner retinal layerwere they connect withboth bipolar and ganglion cells. Understanding their performance is crucial to assess the viability of the inner retina.
First of all, we established the suitable intensity of light for this analysis, and observed that in the late stages of RP the OPs amplitude and frequency decreased, mainly in untreated mice while in myriocin treated retina they were similar to the control wt (3.19). Further, we estimated the area subtended by

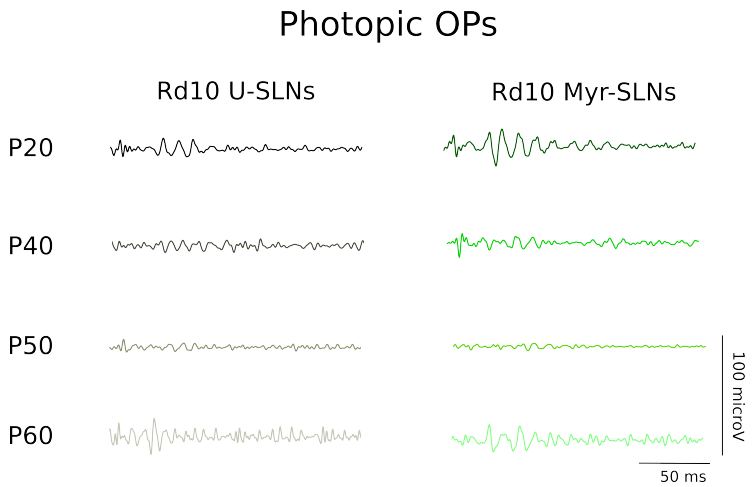

Figure 3.19: OPs from cones photopic ERG responses. The left panel (gray scale) represents the time course of OPs in untreated rd10 retina. The right panel (green scale) represents the same time course in myriocin treated rd10 mice. The OPs amplitude and frequency were improved in treated retinas

the OPs by calculating the integral curve (3.20 A). The results are illustrated in fig. 3.20 B were it is seen that the total OPs area at P60 is significantly larger in myriocin treated retinas.

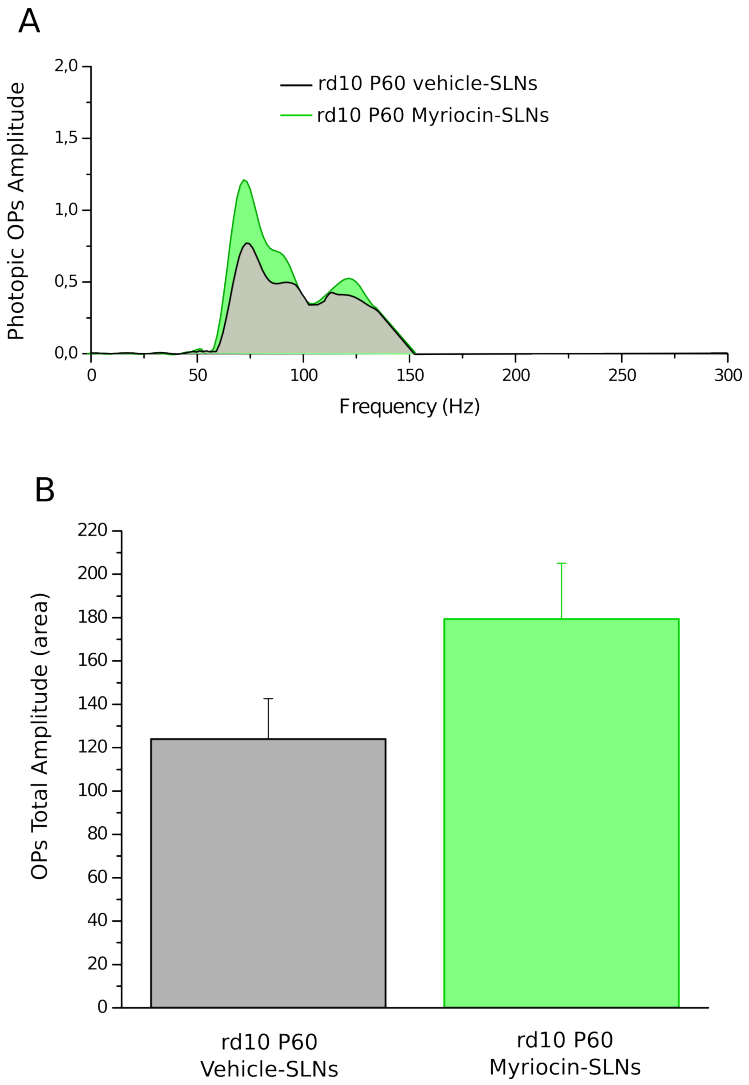

Figure 3.20: Panel A shows an example of curve obtained from OPs analysis; the area under the curve rapresents the total OPs amplitude. The plot bars in the panel B represent the average of four an five animals respectively in control and treated groups. Note that the OPs total area was significantly increased in myriocin treated animals, indicating an improvement in the functional performance of inner retina neurons

Chapter 4

Discussion

4.1 Effects of Myriocin treatment in the early stage of RP

This study demonstrated for the first time that, in the rd10 mouse model of RP, the level of retinal ceramide starts to increase from the third week of life, during the same period of maximum photoreceptor loss, whereas in wild-type mice ceramide levels progressively decrease. Single intraocular injections of myriocin, a selective inhibitor of SPT, the rate-limiting enzyme of ceramide biosynthesis, decreased retinal ceramide and reduced the number of apoptotic photoreceptors in the short term. Functional benefits of myriocin became apparent after prolonged daily treatment, with the ceramide inhibitor caged in solid lipid nanoparticles, non invasively administered as eyedrops. In rd10 mice treated with myriocin-SLNs for 10-20 d, the death of visual cells was slowed, their morphology preserved, and the overall retinal degeneration delayed.
The finding that ceramide levels increase in the rd10 mouse in temporal association with the process of photoreceptors demise provides biochemical evidences that this sphingolipids is involved in the neurodegenerative process of RP ([5], [29]). This results is therefore in accordance with the notion derived from genetic studies that human autosomal recessive RP can be caused by loss-of-function mutations in CERKL, an enzyme that lowers ceramide content by phosphorylation ([4]). The results are also consistent with the increased ceramide levels of other forms ofdystrophy, such as Alzheimer's disease were the cell death occurs by apoptosis ([37]).
In a previous study conducted on a *Drosophila* models of RP ([1]), the increased retinal levels of ceramide were lowered by genetic manipulation, while in this study ceramide levels were lowered pharmacologically. Because a non invasive pharmacological approach is more easily achieved in humans than gene therapy, in the long run, the strategy proposed here might become applicable to humans in the long run.
A functional benefit of myriocin was observed only after prolonged treatment but not after a single intraocular injection, despite the fact that both administration methods reduced ceramide levels. The lack of measurable functional effects of single myriocin administration might be ascribed to the small proportion of photoreceptors rescued from apoptotic death in short period of study (2

d). Possibly the corrisponding effect on the ERG fell below the sensitivity of this functional test.
This study has a few limitations, the most evident being that chronic administration of myriocin rescued a fraction of photoreceptors for a limited period of time, moslty delaying the inevitable death process in these cells. However, it has to be considered that prolonging the natural evolution of a disease like RP, which characteristically exhibits a slow progression, can nontheless represent for patients an important advantage. Another limitation is that we studied a single mutations that leads to RP, whereas it is known that this disease is genetically heterogeneous ([64]).
Overall, the results described here are particularly encouraging, considering that the partial loss-of-function rd10 mutation mimics typical RP forms with moderately aggressive phenotype and good retention of retinal architecture ([29]). These are features that portray human RP patients as likely canididates for gene therapy, in which the defective gene is replaced by a functioning one by means of genetically engineered viral vectors. A protective pharmacological approach, based on the non-invasive administration of SPT inhibitors, could prolong the lifespan of photoreceptors in recessive form of RP, pending gene therapy at a later stage. SPT inhibitors similar to myriocin could therefore contribute to enlarge the panel of bioactive substances already used as neuroprotectants to delay photoreceptors death in this disease ([48], [97]).
Finally, the particular advantages of the SLNs used here are their lack of undesirable effects and their suitability for carrying nonpolar, lipophilic compounds. These features can be exploited for drug delivery in retinal disorders other than RP.
In conclusion, the first step of this study demonstrates that pharmacological targeting of ceramide biosynthesis has the potential to slow the progression of RP in a mammalian models and therefore may represent a therapeutic approach to treating this disease in humans.
Furthermore, considering that an increment in the rate of rod survival is known to promote a proportionally longer viability of cones, essential for daylight vision, it is possible that the beneficial effects of delaying the sphingolipid-mediated rod demise would propagate to cones as well.

4.2 Effects of Myriocin treatment in the later stage of RP

In the rd10 model of retinal degeneration the loss of rod visual cells, in untreated mice, is nearly complete at around P40. At this stage animals may only relay on cone vision that is usually maintained up to no later than P80. Although cone's survival extends well beyond rod's survival, our data show, nonetheless, that signs of functional damage can be detected in cones at the very early stage of rod degeneration. Interestingly, the functional impairment of cones occurs when the structure of these cells is still seemingly normal. Treatment with myriocin rescues rods and also protects cones by partially preventing their functional damage and by significantly prolonging their survival. These observation have important practical consequences because an extension in time of cone viability may be crucial for the applicability and success of some of the most recent therapeutic approaches, and above all, the halorhodopsin-based therapy ([11]).
In rd10 mice as well as in a number of other genetic defects identified in animal's and human's RP the cause of cone degeneration still remains an open question. The main difficulty in understanding this occurrence is that the genetic damage that affects rods seems to spare cones. The prevailing hypothesis in this regard is that cones, to survive, require the presence of rods whose protective action would be exrted through the release of some, not yet indentified, diffusibile factor. In principle this would explain why prolonging rod survival by myriocin also extend cone viability. It must be pointed out, however, that this should not be taken, by all means, as a ruling out of the possibility of a direct action of the drug also on cones. The notion of a direct action of myriocin on cones is supported by the observation that the functional damage, observed in these visual cells at the earliest stages of rod degeneration, may be to some extent reverted by myriocin. The fact that a fuctional damage is already present in cones when rods are still viable arises a number of interesting possibilities. If we assume that rods protect cones by releasing trophic factors, the present results indicate that this action fails as rods start degenerating possibly because the genetic damage also impairs their ability to produce or release the protective molecule. Another possibility is that a subtle as yet undisclosed genetic damage also affects cones.
The cone involvement in retinal degeneration is also puzzling for other reasons. We have shown that the early functional damage of cones in untreated rd10 mice is reflected in the flash ERG where both amplitude and kinetics of the light response are affected. The treatment of these animals with myriocin is effective in restoring the response amplitude near to normal levels, but fails to correct the altered kinetics. It is perhaps important to note that the sole correction of the amplitude does succeed in extending he cone survival but they remain doomed to death and the eventual shedding at the latest stage of retinal degeneration is a warning that protection was not complete, as possibly reflected by the inability of myriocin to also correct the kinetics of the light response.

Bibliography

[1] U. Acharya, S. Patel, E. Koundakjian, K. Nagashima, X. Han, and J. K. Acharya. Modulating sphingolipid biosynthetic pathway rescues photoreceptor degeneration. *Science*, 299(5613):1740–1743, Mar 2003. 1.4, 4.1

[2] R. Adler, K. B. Landa, M. Manthorpe, and S. Varon. Cholinergic neuronotrophic factors: intraocular distribution of trophic activity for ciliary neurons. *Science*, 204(4400):1434–1436, Jun 1979. 1.3.3

[3] G. Alphonse, M. T. Aloy, P. Broquet, J. P. Gerard, P. Louisot, R. Rousson, and C. Rodriguez-Lafrasse. Ceramide induces activation of the mitochondrial/caspases pathway in jurkat and scc61 cells sensitive to gamma-radiation but activation of this sequence is defective in radioresistant sq20b cells. *Int J Radiat Biol*, 78(9):821–835, Sep 2002. 1.4.1

[4] A. Avila-Fernandez, R. Riveiro-Alvarez, E. Vallespin, R. Wilke, I. Tapias, D. Cantalapiedra, J. Aguirre-Lamban, A. Gimenez, M.-J. Trujillo-Tiebas, and C. Ayuso. Cerkl mutations and associated phenotypes in seven spanish families with autosomal recessive retinitis pigmentosa. *Invest Ophthalmol Vis Sci*, 49(6):2709–2713, Jun 2008. 4.1

[5] R. Barhoum, G. Martnez-Navarrete, S. Corrochano, F. Germain, L. Fernandez-Sanchez, E. J. de la Rosa, P. de la Villa, and N. Cuenca. Functional and structural modifications during retinal degeneration in the rd10 mouse. *Neuroscience*, 155(3):698–713, Aug 2008. 4.1

[6] S. Bhattacharya, C. Dooley, F. Soto, J. Madson, A. V. Das, and I. Ahmad. Involvement of ath3 in cntf-mediated differentiation of the late retinal progenitors. *Mol Cell Neurosci*, 27(1):32–43, Sep 2004. 1.3.3

[7] H. Birbes, S. E. Bawab, L. M. Obeid, and Y. A. Hannun. Mitochondria and ceramide: intertwined roles in regulation of apoptosis. *Adv Enzyme Regul*, 42:113–129, 2002. 1.4.1

[8] R. Bose, M. Verheij, A. Haimovitz-Friedman, K. Scotto, Z. Fuks, and R. Kolesnick. Ceramide synthase mediates daunorubicin-induced apoptosis: an alternative mechanism for generating death signals. *Cell*, 82(3):405–414, Aug 1995. 1.4

[9] C. Bowes, T. Li, M. Danciger, L. C. Baxter, M. L. Applebury, and D. B. Farber. Retinal degeneration in the rd mouse is caused by a defect in the beta subunit of rod cgmp-phosphodiesterase. *Nature*, 347(6294):677–680, Oct 1990. 1.2.5

[10] M. E. Breton, A. W. Schueller, T. D. Lamb, and E. N. Pugh. Analysis of erg a-wave amplification and kinetics in terms of the g-protein cascade of phototransduction. *Invest Ophthalmol Vis Sci*, 35(1):295–309, Jan 1994. 1.2.6

[11] V. Busskamp, J. Duebel, D. Balya, M. Fradot, T. J. Viney, S. Siegert, A. C. Groner, E. Cabuy, V. Forster, M. Seeliger, M. Biel, P. Humphries, M. Paques, S. Mohand-Said, D. Trono, K. Deisseroth, J. A. Sahel, S. Picaud, and B. Roska. Genetic reactivation of cone photoreceptors restores visual responses in retinitis pigmentosa. *Science*, 329(5990):413–417, Jul 2010. 1.3.4, 4.2

[12] X. Cao and J. W. Phillis. The free radical scavenger, alpha-lipoic acid, protects against cerebral ischemia-reperfusion injury in gerbils. *Free Radic Res*, 23(4):365–370, Oct 1995. 1.3.5

[13] D. M. Chacko, J. A. Rogers, J. E. Turner, and I. Ahmad. Survival and differentiation of cultured retinal progenitors transplanted in the subretinal space of the rat. *Biochem Biophys Res Commun*, 268(3):842–846, Feb 2000. 1.3.1

[14] B. Chang, N. L. Hawes, R. E. Hurd, M. T. Davisson, S. Nusinowitz, and J. R. Heckenlively. Retinal degeneration mutants in the mouse. *Vision Res*, 42(4):517–525, Feb 2002. 1.2.5, 1.2.5, 1.2.6, 2.1

[15] B. Chang, N. L. Hawes, M. T. Pardue, A. M. German, R. E. Hurd, M. T. Davisson, S. Nusinowitz, K. Rengarajan, A. P. Boyd, S. S. Sidney, M. J. Phillips, R. E. Stewart, R. Chaudhury, J. M. Nickerson, J. R. Heckenlively, and J. H. Boatright. Two mouse retinal degenerations caused by missense mutations in the beta-subunit of rod cgmp phosphodiesterase gene. *Vision Res*, 47(5):624–633, Mar 2007. 1.2.6

[16] G. Q. Chang, Y. Hao, and F. Wong. Apoptosis: final common pathway of photoreceptor death in rd, rds, and rhodopsin mutant mice. *Neuron*, 11(4):595–605, Oct 1993. 1.2.5

[17] S. Chen, Q.-L. Wang, S. Xu, I. Liu, L. Y. Li, Y. Wang, and D. J. Zack. Functional analysis of cone-rod homeobox (crx) mutations associated with retinal dystrophy. *Hum Mol Genet*, 11(8):873–884, Apr 2002. 1.2.4

[18] V. Chrysostomou, J. Stone, S. Stowe, N. L. Barnett, and K. Valter. The status of cones in the rhodopsin mutant p23h-3 retina: light-regulated damage and repair in parallel with rods. *Invest Ophthalmol Vis Sci*, 49(3):1116–1125, Mar 2008. 1.2.7

[19] B. L. K. Coles, B. Angnieux, T. Inoue, K. D. Rio-Tsonis, J. R. Spence, R. R. McInnes, Y. Arsenijevic, and D. van der Kooy. Facile isolation and the characterization of human retinal stem cells. *Proc Natl Acad Sci U S A*, 101(44):15772–15777, Nov 2004. 1.3.1

[20] O. Cuvillier, G. Pirianov, B. Kleuser, P. G. Vanek, O. A. Coso, S. Gutkind, and S. Spiegel. Suppression of ceramide-mediated programmed cell death by sphingosine-1-phosphate. *Nature*, 381(6585):800–803, Jun 1996. 1.4.1

[21] G. C. Demontis, A. Sbrana, C. Gargini, and L. Cervetto. A simple and inexpensive light source for research in visual neuroscience. *J Neurosci Methods*, 146(1):13–21, Jul 2005. 2.6.2

[22] T. P. Dryja, T. L. McGee, E. Reichel, L. B. Hahn, G. S. Cowley, D. W. Yandell, M. A. Sandberg, and E. L. Berson. A point mutation of the rhodopsin gene in one form of retinitis pigmentosa. *Nature*, 343(6256):364–366, Jan 1990. 1.3.3

[23] Z. D. Ezzeddine, X. Yang, T. DeChiara, G. Yancopoulos, and C. L. Cepko. Postmitotic cells fated to become rod photoreceptors can be respecified by cntf treatment of the retina. *Development*, 124(5):1055–1067, Mar 1997. 1.3.3

[24] E. G. Faktorovich, R. H. Steinberg, D. Yasumura, M. T. Matthes, and M. M. LaVail. Photoreceptor degeneration in inherited retinal dystrophy delayed by basic fibroblast growth factor. *Nature*, 347(6288):83–86, Sep 1990. 1.3.3

[25] D. B. Farber, J. R. Heckenlively, R. S. Sparkes, and J. B. Bateman. Molecular genetics of retinitis pigmentosa. *West J Med*, 155(4):388–399, Oct 1991. 1.2.5

[26] G. J. Farrar, P. Kenna, S. A. Jordan, R. Kumar-Singh, M. M. Humphries, E. M. Sharp, D. M. Sheils, and P. Humphries. A three-base-pair deletion in the peripherin-rds gene in one form of retinitis pigmentosa. *Nature*, 354(6353):478–480, Dec 1991. 1.2.3

[27] S. Fuhrmann, M. Kirsch, and H. D. Hofmann. Ciliary neurotrophic factor promotes chick photoreceptor development in vitro. *Development*, 121(8):2695–2706, Aug 1995. 1.3.3

[28] A. Gal, U. Orth, W. Baehr, E. Schwinger, and T. Rosenberg. Heterozygous missense mutation in the rod cgmp phosphodiesterase beta-subunit gene in autosomal dominant stationary night blindness. *Nat Genet*, 7(1):64–68, May 1994. 1.2.5

[29] C. Gargini, E. Terzibasi, F. Mazzoni, and E. Strettoi. Retinal organization in the retinal degeneration 10 (rd10) mutant mouse: a morphological and erg study. *J Comp Neurol*, 500(2):222–238, Jan 2007. 1.2.6, 2.3.2, 3.3, 4.1

[30] P. Goldsmith, H. Baier, and W. A. Harris. Two zebrafish mutants, ebony and ivory, uncover benefits of neighborhood on photoreceptor survival. *J Neurobiol*, 57(3):235–245, Dec 2003. 1.3.3

[31] V. Gouaz, M. E. Mirault, S. Carpentier, R. Salvayre, T. Levade, and N. Andrieu-Abadie. Glutathione peroxidase-1 overexpression prevents ceramide production and partially inhibits apoptosis in doxorubicin-treated human breast carcinoma cells. *Mol Pharmacol*, 60(3):488–496, Sep 2001. 1.4

[32] P. Gouras, J. Du, H. Kjeldbye, R. Kwun, R. Lopez, and D. J. Zack. Transplanted photoreceptors identified in dystrophic mouse retina by a transgenic reporter gene. *Invest Ophthalmol Vis Sci*, 32(13):3167–3174, Dec 1991. 1.3.1

[33] P. Gouras, J. Du, H. Kjeldbye, S. Yamamoto, and D. J. Zack. Long-term photoreceptor transplants in dystrophic and normal mouse retina. *Invest Ophthalmol Vis Sci*, 35(8):3145–3153, Jul 1994. 1.3.1

[34] O. Goureau, K. D. Rhee, and X.-J. Yang. Ciliary neurotrophic factor promotes muller glia differentiation from the postnatal retinal progenitor pool. *Dev Neurosci*, 26(5-6):359–370, 2004. 1.3.3

[35] Y. A. Hannun. Functions of ceramide in coordinating cellular responses to stress. *Science*, 274(5294):1855–1859, Dec 1996. 1.4.1

[36] Y. A. Hannun, C. Luberto, and K. M. Argraves. Enzymes of sphingolipid metabolism: from modular to integrative signaling. *Biochemistry*, 40(16):4893–4903, Apr 2001. 1.4

[37] B. He, N. Lu, and Z. Zhou. Cellular and nuclear degradation during apoptosis. *Curr Opin Cell Biol*, 21(6):900–912, Dec 2009. 4.1

[38] A. T. Hewitt, J. D. Lindsey, D. Carbott, and R. Adler. Photoreceptor survival-promoting activity in interphotoreceptor matrix preparations: characterization and partial purification. *Exp Eye Res*, 50(1):79–88, Jan 1990. 1.3.3

[39] P. C. Huang, A. E. Gaitan, Y. Hao, R. M. Petters, and F. Wong. Cellular interactions implicated in the mechanism of photoreceptor degeneration in transgenic mice expressing a mutant rhodopsin gene. *Proc Natl Acad Sci U S A*, 90(18):8484–8488, Sep 1993. 1.3.3

[40] M. A. Ionita and S. J. Pittler. Focus on molecules: rod cgmp phosphodiesterase type 6. *Exp Eye Res*, 84(1):1–2, Jan 2007. 1.2.5

[41] S. A. Jo, E. Wang, and L. I. Benowitz. Ciliary neurotrophic factor is an axogenesis factor for retinal ganglion cells. *Neuroscience*, 89(2):579–591, Mar 1999. 1.3.3

[42] K. Kajiwara, L. B. Hahn, S. Mukai, G. H. Travis, E. L. Berson, and T. P. Dryja. Mutations in the human retinal degeneration slow gene in autosomal dominant retinitis pigmentosa. *Nature*, 354(6353):480–483, Dec 1991. 1.2.3

[43] C. E. Keeler. The inheritance of a retinal abnormality in white mice. *Proc Natl Acad Sci U S A*, 10(7):329–333, Jul 1924. 1.2.5

[44] A. Kennan, A. Aherne, and P. Humphries. Light in retinitis pigmentosa. *Trends Genet*, 21(2):103–110, Feb 2005. 1.2

[45] M. Kirsch, S. Fuhrmann, A. Wiese, and H. D. Hofmann. Cntf exerts opposite effects on in vitro development of rat and chick photoreceptors. *Neuroreport*, 7(3):697–700, Feb 1996. 1.3.3

[46] H. Klassen, D. S. Sakaguchi, and M. J. Young. Stem cells and retinal repair. *Prog Retin Eye Res*, 23(2):149–181, Mar 2004. 1.3.1

[47] R. N. Kolesnick and M. Krnke. Regulation of ceramide production and apoptosis. *Annu Rev Physiol*, 60:643–665, 1998. 1.4.1

[48] K. Komeima, B. S. Rogers, L. Lu, and P. A. Campochiaro. Antioxidants reduce cone cell death in a model of retinitis pigmentosa. *Proc Natl Acad Sci U S A*, 103(30):11300–11305, Jul 2006. 1.3.5, 4.1

[49] R. A. Kowluru and S. Odenbach. Effect of long-term administration of alpha-lipoic acid on retinal capillary cell death and the development of retinopathy in diabetic rats. *Diabetes*, 53(12):3233–3238, Dec 2004. 1.3.5

[50] R. R. Lakhanpal, D. Yanai, J. D. Weiland, G. Y. Fujii, S. Caffey, R. J. Greenberg, E. de Juan, and M. S. Humayun. Advances in the development of visual prostheses. *Curr Opin Ophthalmol*, 14(3):122–127, Jun 2003. 1.3.2

[51] M. M. LaVail, D. Yasumura, M. T. Matthes, C. Lau-Villacorta, K. Unoki, C. H. Sung, and R. H. Steinberg. Protection of mouse photoreceptors by survival factors in retinal degenerations. *Invest Ophthalmol Vis Sci*, 39(3):592–602, Mar 1998. 1.3.3

[52] B. Lei, G. Yao, K. Zhang, K. J. Hofeldt, and B. Chang. Study of rod- and cone-driven oscillatory potentials in mice. *Invest Ophthalmol Vis Sci*, 47(6):2732–2738, Jun 2006. 2.6.3

[53] Y. Li, W. Tao, L. Luo, D. Huang, K. Kauper, P. Stabila, M. M. Lavail, A. M. Laties, and R. Wen. Cntf induces regeneration of cone outer segments in a rat model of retinal degeneration. *PLoS One*, 5(3):e9495, 2010. 1.3.3

[54] C.-F. Lin, C.-L. Chen, W.-T. Chang, M.-S. Jan, L.-J. Hsu, R.-H. Wu, M.-J. Tang, W.-C. Chang, and Y.-S. Lin. Sequential caspase-2 and caspase-8 activation upstream of mitochondria during ceramideand etoposide-induced apoptosis. *J Biol Chem*, 279(39):40755–40761, Sep 2004. 1.4.1

[55] L. F. Lin, D. Mismer, J. D. Lile, L. G. Armes, E. T. Butler, J. L. Vannice, and F. Collins. Purification, cloning, and expression of ciliary neurotrophic factor (cntf). *Science*, 246(4933):1023–1025, Nov 1989. 1.3.3

[56] S. C. Linn, H. S. Kim, E. M. Keane, L. M. Andras, E. Wang, and A. H. Merrill. Regulation of de novo sphingolipid biosynthesis and the toxic consequences of its disruption. *Biochem Soc Trans*, 29(Pt 6):831–835, Nov 2001. 1.4

[57] C. J. R. Loewen, O. L. Moritz, B. M. Tam, D. S. Papermaster, and R. S. Molday. The role of subunit assembly in peripherin-2 targeting to rod photoreceptor disk membranes and retinitis pigmentosa. *Mol Biol Cell*, 14(8):3400–3413, Aug 2003. 1.2.3

[58] A. L. Lyubarsky, L. L. Daniele, and E. N. Pugh. From candelas to photoisomerizations in the mouse eye by rhodopsin bleaching in situ and the light-rearing dependence of the major components of the mouse ERG. *Vision Res*, 44(28):3235–3251, Dec 2004. 2.6.2

[59] A. L. Lyubarsky and E. N. Pugh. Recovery phase of the murine rod photoresponse reconstructed from electroretinographic recordings. *J Neurosci*, 16(2):563–571, Jan 1996. 2.6.2

[60] T. Lveillard, S. Mohand-Sad, O. Lorentz, D. Hicks, A.-C. Fintz, E. Clrin, M. Simonutti, V. Forster, N. Cavusoglu, F. Chalmel, P. Doll, O. Poch, G. Lambrou, and J.-A. Sahel. Identification and characterization of rod-derived cone viability factor. *Nat Genet*, 36(7):755–759, Jul 2004. 1.3.3

[61] R. E. MacLaren, R. A. Pearson, A. MacNeil, R. H. Douglas, T. E. Salt, M. Akimoto, A. Swaroop, J. C. Sowden, and R. R. Ali. Retinal repair by transplantation of photoreceptor precursors. *Nature*, 444(7116):203–207, Nov 2006. 1.3.1

[62] E. C. Mandon, I. Ehses, J. Rother, G. van Echten, and K. Sandhoff. Subcellular localization and membrane topology of serine palmitoyltransferase, 3-dehydrosphinganine reductase, and sphinganine n-acyltransferase in mouse liver. *J Biol Chem*, 267(16):11144–11148, Jun 1992. 1.4.1

[63] W. F. Marasas. Discovery and occurrence of the fumonisins: a historical perspective. *Environ Health Perspect*, 109 Suppl 2:239–243, May 2001. 1.4.2

[64] V. Marigo. Programmed cell death in retinal degeneration: targeting apoptosis in photoreceptors as potential therapy for retinal degeneration. *Cell Cycle*, 6(6):652–655, Mar 2007. 4.1

[65] M. E. McLaughlin, T. L. Ehrhart, E. L. Berson, and T. P. Dryja. Mutation spectrum of the gene encoding the beta subunit of rod phosphodiesterase among patients with autosomal recessive retinitis pigmentosa. *Proc Natl Acad Sci U S A*, 92(8):3249–3253, Apr 1995. 1.2.5

[66] M. E. McLaughlin, M. A. Sandberg, E. L. Berson, and T. P. Dryja. Recessive mutations in the gene encoding the beta-subunit of rod phosphodiesterase in patients with retinitis pigmentosa. *Nat Genet*, 4(2):130–134, Jun 1993. 1.2.5

[67] S. Melov, J. A. Schneider, B. J. Day, D. Hinerfeld, P. Coskun, S. S. Mirra, J. D. Crapo, and D. C. Wallace. A novel neurological phenotype in mice lacking mitochondrial manganese superoxide dismutase. *Nat Genet*, 18(2):159–163, Feb 1998. 1.3.5

[68] H. F. Mendes, J. van der Spuy, J. P. Chapple, and M. E. Cheetham. Mechanisms of cell death in rhodopsin retinitis pigmentosa: implications for therapy. *Trends Mol Med*, 11(4):177–185, Apr 2005. 1.2, 1.2.1

[69] A. Meyer-Franke, M. R. Kaplan, F. W. Pfrieger, and B. A. Barres. Characterization of the signaling interactions that promote the survival and growth of developing retinal ganglion cells in culture. *Neuron*, 15(4):805–819, Oct 1995. 1.3.3

[70] Y. Miyake, Y. Kozutsumi, S. Nakamura, T. Fujita, and T. Kawasaki. Serine palmitoyltransferase is the primary target of a sphingosine-like immunosuppressant, isp-1/myriocin. *Biochem Biophys Res Commun*, 211(2):396–403, Jun 1995. 1.4.2

[71] D. Mustafi, A. H. Engel, and K. Palczewski. Structure of cone photoreceptors. *Prog Retin Eye Res*, 28(4):289–302, Jul 2009. 1.2.7, 3.3.2

[72] C. Neophytou, A. B. Vernallis, A. Smith, and M. C. Raff. Mller-cell-derived leukaemia inhibitory factor arrests rod photoreceptor differentiation at a postmitotic pre-rod stage of development. *Development*, 124(12):2345–2354, Jun 1997. 1.3.3

[73] B. Nespereira, M. Prez-Ilzarbe, P. Fernndez, A. M. Fuentes, J. A. Pramo, and J. A. Rodrguez. Vitamins c and e downregulate vascular vegf and vegfr-2 expression in apolipoprotein-e-deficient mice. *Atherosclerosis*, 171(1):67–73, Nov 2003. 1.3.5

[74] S. A. Novgorodov, T. I. Gudz, and L. M. Obeid. Long-chain ceramide is a potent inhibitor of the mitochondrial permeability transition pore. *J Biol Chem*, 283(36):24707–24717, Sep 2008. 1.4.1

[75] L. M. Obeid, C. M. Linardic, L. A. Karolak, and Y. A. Hannun. Programmed cell death induced by ceramide. *Science*, 259(5102):1769–1771, Mar 1993. 1.4.1

[76] A. Olivera and S. Spiegel. Sphingosine-1-phosphate as second messenger in cell proliferation induced by pdgf and fcs mitogens. *Nature*, 365(6446):557–560, Oct 1993. 1.4.1

[77] J. E. Olsson, J. W. Gordon, B. S. Pawlyk, D. Roof, A. Hayes, R. S. Molday, S. Mukai, G. S. Cowley, E. L. Berson, and T. P. Dryja. Transgenic mice with a rhodopsin mutation (pro23his): a mouse model of autosomal dominant retinitis pigmentosa. *Neuron*, 9(5):815–830, Nov 1992. 1.2.2

[78] A. Otani, M. I. Dorrell, K. Kinder, S. K. Moreno, S. Nusinowitz, E. Banin, J. Heckenlively, and M. Friedlander. Rescue of retinal degeneration by intravitreally injected adult bone marrow-derived lineage-negative hematopoietic stem cells. *J Clin Invest*, 114(6):765–774, Sep 2004. 1.3.1

[79] Y. A. Ovchinnikov. Structure of rhodopsin and bacteriorhodopsin. *Photochem Photobiol*, 45(6):909–914, Jun 1987. 1.2.2

[80] Y. A. Ovchinnikov, N. G. Abdulaev, M. Y. Feigina, A. V. Kiselev, and N. A. Lobanov. The structural basis of the functioning of bacteriorhodopsin: an overview. *FEBS Lett*, 100(2):219–224, Apr 1979. 1.2.2

[81] D. M. Paskowitz, M. M. LaVail, and J. L. Duncan. Light and inherited retinal degeneration. *Br J Ophthalmol*, 90(8):1060–1066, Aug 2006. 1.2

[82] E. Passage, J. C. Norreel, P. Noack-Fraissignes, V. Sanguedolce, J. Pizant, X. Thirion, A. Robaglia-Schlupp, J. F. Pellissier, and M. Fonts. Ascorbic acid treatment corrects the phenotype of a mouse model of charcot-marie-tooth disease. *Nat Med*, 10(4):396–401, Apr 2004. 1.3.5

[83] R. M. Petters, C. A. Alexander, K. D. Wells, E. B. Collins, J. R. Sommer, M. R. Blanton, G. Rojas, Y. Hao, W. L. Flowers, E. Banin, A. V. Cideciyan, S. G. Jacobson, and F. Wong. Genetically engineered large animal model for studying cone photoreceptor survival and degeneration in retinitis pigmentosa. *Nat Biotechnol*, 15(10):965–970, Oct 1997. 1.3.3

[84] S. J. Pittler and W. Baehr. Identification of a nonsense mutation in the rod photoreceptor cgmp phosphodiesterase beta-subunit gene of the rd mouse. *Proc Natl Acad Sci U S A*, 88(19):8322–8326, Oct 1991. 1.2.5

[85] S. J. Pittler and W. Baehr. The molecular genetics of retinal photoreceptor proteins involved in cgmp metabolism. *Prog Clin Biol Res*, 362:33–66, 1991. 1.2.5

[86] S. J. Pittler, C. E. Keeler, R. L. Sidman, and W. Baehr. Pcr analysis of dna from 70-year-old sections of rodless retina demonstrates identity with the mouse rd defect. *Proc Natl Acad Sci U S A*, 90(20):9616–9619, Oct 1993. 1.2.5

[87] T. Puthussery, J. Gayet-Primo, S. Pandey, R. M. Duvoisin, and W. R. Taylor. Differential loss and preservation of glutamate receptor function in bipolar cells in the rd10 mouse model of retinitis pigmentosa. *Eur J Neurosci*, 29(8):1533–1542, Apr 2009. 3.3.2

[88] L. Riboni, R. Campanella, R. Bassi, R. Villani, S. M. Gaini, F. Martinelli-Boneschi, P. Viani, and G. Tettamanti. Ceramide levels are inversely associated with malignant progression of human glial tumors. *Glia*, 39(2):105–113, Aug 2002. 1.4.1

[89] J. A. Sahel, S. Mohand-Said, T. Lveillard, D. Hicks, S. Picaud, and H. Dreyfus. Rod-cone interdependence: implications for therapy of photoreceptor cell diseases. *Prog Brain Res*, 131:649–661, 2001. 1.2.7, 3.3.2

[90] J. Sancho-Pelluz, B. Arango-Gonzalez, S. Kustermann, F. J. Romero, T. van Veen, E. Zrenner, P. Ekstrm, and F. Paquet-Durand. Photoreceptor cell death mechanisms in inherited retinal degeneration. *Mol Neurobiol*, 38(3):253–269, Dec 2008. 1.2.5

[91] N. Sanvicens and T. G. Cotter. Ceramide is the key mediator of oxidative stress-induced apoptosis in retinal photoreceptor cells. *J Neurochem*, 98(5):1432–1444, Sep 2006. 2.5

[92] S. Schulz-Key, H.-D. Hofmann, C. Beisenherz-Huss, C. Barbisch, and M. Kirsch. Ciliary neurotrophic factor as a transient negative regulator of rod development in rat retina. *Invest Ophthalmol Vis Sci*, 43(9):3099–3108, Sep 2002. 1.3.3

[93] M. Seiler, R. B. Aramant, B. Ehinger, and A. R. Adolph. Transplantation of embryonic retina to adult retina in rabbits. *Exp Eye Res*, 51(2):225–228, Aug 1990. 1.3.1

[94] J. Shen, X. Yang, A. Dong, R. M. Petters, Y.-W. Peng, F. Wong, and P. A. Campochiaro. Oxidative damage is a potential cause of cone cell death in retinitis pigmentosa. *J Cell Physiol*, 203(3):457–464, Jun 2005. 1.2.7

[95] M. Shimabukuro, M. Higa, Y. T. Zhou, M. Y. Wang, C. B. Newgard, and R. H. Unger. Lipoapoptosis in beta-cells of obese prediabetic fa/fa rats. role of serine palmitoyltransferase overexpression. *J Biol Chem*, 273(49):32487–32490, Dec 1998. 1.4.2

[96] H. Shimeno, S. Soeda, M. Sakamoto, T. Kouchi, T. Kowakame, and T. Kihara. Partial purification and characterization of sphingosine n-acyltransferase (ceramide synthase) from bovine liver mitochondrion-rich fraction. *Lipids*, 33(6):601–605, Jun 1998. 1.4.1

[97] P. A. Sieving, R. C. Caruso, W. Tao, H. R. Coleman, D. J. S. Thompson, K. R. Fullmer, and R. A. Bush. Ciliary neurotrophic factor (cntf) for human retinal degeneration: phase i trial of cntf delivered by encapsulated cell intraocular implants. *Proc Natl Acad Sci U S A*, 103(10):3896–3901, Mar 2006. 1.3.3, 4.1

[98] S. M. Somani, K. Husain, C. Whitworth, G. L. Trammell, M. Malafa, and L. P. Rybak. Dose-dependent protection by lipoic acid against cisplatin-induced nephrotoxicity in rats: antioxidant defense system. *Pharmacol Toxicol*, 86(5):234–241, May 2000. 1.3.5

[99] B. A. Stoica, V. A. Movsesyan, P. M. Lea, and A. I. Faden. Ceramide-induced neuronal apoptosis is associated with dephosphorylation of akt, bad, fkhr, gsk-3beta, and induction of the mitochondrial-dependent intrinsic caspase pathway. *Mol Cell Neurosci*, 22(3):365–382, Mar 2003. 1.4.1

[100] D. A. Stoyanovsky, R. Goldman, R. M. Darrow, D. T. Organisciak, and V. E. Kagan. Endogenous ascorbate regenerates vitamin e in the retina directly and in combination with exogenous dihydrolipoic acid. *Curr Eye Res*, 14(3):181–189, Mar 1995. 1.3.5

[101] E. Strettoi, C. Gargini, E. Novelli, G. Sala, I. Piano, P. Gasco, and R. Ghidoni. Inhibition of ceramide biosynthesis preserves photoreceptor structure and function in a mouse model of retinitis pigmentosa. *Proc Natl Acad Sci U S A*, 107(43):18706–18711, Oct 2010. 2.3.2, 3.2.2, 3.2.2

[102] K. A. Stckli, F. Lottspeich, M. Sendtner, P. Masiakowski, P. Carroll, R. Gtz, D. Lindholm, and H. Thoenen. Molecular cloning, expression and regional distribution of rat ciliary neurotrophic factor. *Nature*, 342(6252):920–923, 1989. 1.3.3

[103] Y. Sun, R. Taniguchi, D. Tanoue, T. Yamaji, H. Takematsu, K. Mori, T. Fujita, T. Kawasaki, and Y. Kozutsumi. Sli2 (ypk1), a homologue of mammalian protein kinase sgk, is a downstream kinase in the sphingolipid-mediated signaling pathway of yeast. *Mol Cell Biol*, 20(12):4411–4419, Jun 2000. 1.4.2

[104] M. Tuson, G. Marfany, and R. Gonzlez-Duarte. Mutation of cerkl, a novel human ceramide kinase gene, causes autosomal recessive retinitis pigmentosa (rp26). *Am J Hum Genet*, 74(1):128–138, Jan 2004. 1.4

[105] S. Varon, M. Manthorpe, and R. Adler. Cholinergic neuronotrophic factors: I. survival, neurite outgrowth and choline acetyltransferase activity in monolayer cultures from chick embryo ciliary ganglia. *Brain Res*, 173(1):29–45, Sep 1979. 1.3.3

[106] L. Wachtmeister. Oscillatory potentials in the retina: what do they reveal. *Prog Retin Eye Res*, 17(4):485–521, Oct 1998. 2.6.3

[107] D. Y. Wang, W. M. Chan, P. O. S. Tam, L. Baum, D. S. C. Lam, K. K. L. Chong, B. J. Fan, and C. P. Pang. Gene mutations in retinitis pigmentosa and their clinical implications. *Clin Chim Acta*, 351(1-2):5–16, Jan 2005. 1.2.3

[108] J. Weise, S. Isenmann, N. Klcker, S. Kgler, S. Hirsch, C. Gravel, and M. Bhr. Adenovirus-mediated expression of ciliary neurotrophic factor (cntf) rescues axotomized rat retinal ganglion cells but does not support axonal regeneration in vivo. *Neurobiol Dis*, 7(3):212–223, Jun 2000. 1.3.3

[109] R. Wen, Y. Song, S. Kjellstrom, A. Tanikawa, Y. Liu, Y. Li, L. Zhao, R. A. Bush, A. M. Laties, and P. A. Sieving. Regulation of rod phototransduction machinery by ciliary neurotrophic factor. *J Neurosci*, 26(52):13523–13530, Dec 2006. 1.3.3

[110] R. Wen, Y. Song, Y. Liu, Y. Li, L. Zhao, and A. M. Laties. Cntf negatively regulates the phototransduction machinery in rod photoreceptors: implication for light-induced photostasis plasticity. *Adv Exp Med Biol*, 613:407–413, 2008. 1.3.3

[111] H. Q. Xie and R. Adler. Green cone opsin and rhodopsin regulation by cntf and staurosporine in cultured chick photoreceptors. *Invest Ophthalmol Vis Sci*, 41(13):4317–4323, Dec 2000. 1.3.3

[112] Y. Yang, S. Mohand-Said, A. Danan, M. Simonutti, V. Fontaine, E. Clerin, S. Picaud, T. Lveillard, and J.-A. Sahel. Functional cone rescue by rdcvf protein in a dominant model of retinitis pigmentosa. *Mol Ther*, 17(5):787–795, May 2009. 1.2.7, 1.3.3

[113] C. Zhang, J.-K. Shen, T. T. Lam, H.-Y. Zeng, S. K. Chiang, F. Yang, and M. O. M. Tso. Activation of microglia and chemokines in light-induced retinal degeneration. *Mol Vis*, 11:887–895, 2005. 1.2.7

[114] K. Zhang, G. Yao, Y. Gao, K. J. Hofeldt, and B. Lei. Frequency spectrum and amplitude analysis of dark- and light-adapted oscillatory potentials in albino mouse, rat and rabbit. *Doc Ophthalmol*, 115(2):85–93, Sep 2007. 2.6.3

[115] Y. Zhang, K. Arnr, B. Ehinger, and M.-T. R. Perez. Limitation of anatomical integration between subretinal transplants and the host retina. *Invest Ophthalmol Vis Sci*, 44(1):324–331, Jan 2003. 1.3.1

[116] E. Zrenner. The subretinal implant: can microphotodiode arrays replace degenerated retinal photoreceptors to restore vision? *Ophthalmologica*, 216 Suppl 1:8–20; discussion 52–3, 2002. 1.3.2